The transcription factor TCF7L2 functions as a terminal selector in thalamic and habenular regions of the brain

Marcin Andrzej Lipiec,[1,2] Kamil Koziński,[1] Tomasz Zajkowski,[1] Michał Dąbrowski,[3] Chaitali Chakraborty,[1] Angel Toval,[4] José Luis Ferran,[4] Andrzej Nagalski,[1] Marta Barbara Wiśniewska[1,*]

1. Centre of New Technologies, University of Warsaw, Poland
2. Faculty of Biology, University of Warsaw, Poland
3. Nencki Institute of Experimental Biology, Warsaw, Poland
4. Department of Human Anatomy and Psychobiology, School of Medicine, University of Murcia, Spain

*Correspondence should be addressed to Marta B. Wiśniewska, Centre of New Technologies, University of Warsaw; m.wisniewska@cent.uw.edu.pl

Keywords

thalamus, habenula, TCF7L2, Wnt signalling, transcription factor, terminal selector, brain development, postmitotic differentiation, maintenance, neuronal identity

Abstract

Background

The thalamus and habenula integrate sensory information, adaptive task control, and reward processing. Their postmitotic differentiation is not fully understood, information which is essential for elucidating the aetiology of thalamic and habenular dysfunctions seen in multiple neuropsychiatric disorders. Here, we have used mouse models to investigate the function of the thalamo-habenular-specific transcription factor TCF7L2 in the development and maintaining of this region.

Results

In *Tcf7l2* knockout embryos, the later developmental expression of the pan-thalamic and pan-habenular selectors *Gbx2* and *Pou4f1*, respectively, was down-regulated, as were subregional transcription factor, cell adhesion and axon guidance genes. Neurons in the thalamo-habenular region did not segregate to form separate nuclei, did not grow axons toward their targets, and their afferent connections were disorganised. Post-developmental knockout of *Tcf7l2* mildly affected thalamic patterning. Although generic glutamatergic neurotransmitter identity of the thalamo-habenular domain was properly established and maintained in both mutant mice, numerous region-specific synaptic transmission genes that shape neuronal excitability were down-regulated.

Conclusion

TCF7L2 functions as a vertebrate terminal selector, orchestrating a network of transcription factor genes to regulate thalamo-habenular postmitotic molecular differentiation and maintaining terminal differentiation programs.

Background

In the vertebrate forebrain the thalamus and habenula are derived from the alar plate of prosomere 2 in the diencephalon [1, 2]. The thalamus is a sensory relay centre, and part of the cortico-subcortical neural loops that process sensorimotor information and produce goal-directed behaviours [3-5]. The habenula controls reward- and aversion-driven behaviours by connecting the prefrontal cortex, limbic system, and basal ganglia with the monoamine system in the brainstem [6, 7]. Anatomical abnormalities and disconnectivity of the thalamus and habenula are implicated in schizophrenia, autism spectrum disorder, Tourette syndrome, obsessive-compulsive disorder, and depression [8-10]. Knowledge of thalamic and habenular development is required to fully understand the aetiology of these psychiatric conditions, but such information is currently limited.

TCF7L2 is a member of the LEF1/TCF family of transcription factors that cooperates with β-catenin in the canonical Wnt signalling pathway [11]. TCF7L2 polymorphisms have been associated with bipolar disorder, schizophrenia and autism [12-16], and TCF7L2-deficient mice and zebrafish exhibited altered behavioural responses [17, 18]. TCF7L2 is highly and specifically expressed in the thalamus, habenula, pretectum, and some mesencephalic regions [19-21]. Expression of *Tcf7l2* is induced in progenitors of prosomere 2, and high levels of TCF7L2 protein is observed in postmitotic neurons [22, 23]. The majority of regions that are derived from prosomere 2 express *Tcf7l2* throughout life. *Tcf7l2* expression is down-regulated later in development only in the most rostral part of the thalamus (rTh) [19, 24], a small region that give rise to a small population of γ-aminobutyric acid (GABA)-ergic interneurons [25-27]. Wnt/β-catenin signalling and its effectors regulate neuronal fate specification and neurogenesis in different parts of the brain [28-34]. In the diencephalic region of the neural tube, the canonical

Wnt pathway plays a role in the formation of the zona limitans intrathalamica (ZLI) [35-39], an important forebrain signalling centre, that function as a local organiser of thalamic development. [38, 40-42]. However, this early functions of Wnt signalling are not mediated by TCF7L2, because the knockout of *Tcf7l2* had no effect on proliferation or specification of prosomere 2 progenitors in mice and zebrafish [23, 43], consistent with the induction of *Tcf7l2* expression only during neurogenesis.

During postmitotic differentiation, thalamic and habenular neurons extend axons toward their targets [44-46], segregate into discrete nuclei, and develop specific molecular identities [24, 47-51]. These processes are presumably regulated by prosomere 2-specific postmitotic transcription factors. *Tcf7l2* is the only shared marker of both the thalamus and habenula. *Gbx2* is an early specific marker of the thalamic mantle zone, except of the rTh, whereas the expression of *Pou4f1* marks postmitotic habenula neurons [52]. In addition to *Gbx2*, *Pou4f1*, and *Tcf7l2*, newly generated prosomere 2 neurons in different subregions induce the expression of several dozen transcription factor genes, such as *Rora*, *Foxp2*, *Prox1*, *Etv1*, *Nr4a2*, *Hopx*, and *Lef1* [24, 28, 48, 52-55].

Among thalamus-specific transcription factors, only GBX2 has been thoroughly investigated during postmitotic differentiation of the thalamus. GBX2 represses habenular identity in the developing thalamus [56] and promotes the survival of neurons in a subset of thalamic nuclei [57]. GBX2 is involved in the establishment of thalamic axon trajectories [58-60] and plays a role in anatomical boundary formation within the diencephalon [61]. The habenula-specific marker POU4F1 is required for the establishment and maintenance of habenular identity, survival of neurons, and growth of the fasciculus retroflexus [52, 62]. Few studies have investigated the role of postmitotic transcription factor markers expressed in subregions of the thalamus and

habenula during development: RORA [63], FOXP2 [64], and NR4A2 [52]. *Rora, Foxp2* and *Nr4a2* mutations have mainly local, less severe effects. The function of TCF7L2 in the postmitotic development of thalamic and habenular regions has only begun to be elucidated. Postmitotic precursors of the ventral habenula in *tcf7l2* mutant zebrafish did not migrate properly [65], and neurons of the dorsal habenula did not adopt asymmetrical identities [43]. In *Tcf7l2*$^{-/-}$ mice, some postmitotic markers were mis-expressed in the prospective thalamus and habenula during neurogenesis and the formation of habenulo-interpeduncular tract was disrupted [23]. The role of TCF7L2 during the later clustering of neurons and terminal differentiation has not been investigated.

Here, we have used complete and conditional knockouts in mice to investigate the role of *Tcf7l2* during neurogenesis and in the adult brain. We show that TCF7L2 maintains *Gbx2* and *Pou4f1* expression, coordinates the expression of a network of subregion-specific transcription factors, and controls nucleogenesis in prosomere 2. TCF7L2 also regulates morphological and functional connectivity of the thalamus and habenula. In addition to the establishment of axonal connections, TCF7L2 is required for the acquisition and maintenance in adults of electrophysiological identities in the thalamo-habenular domain.

Results

Normal neurogenesis and disrupted regional anatomy in prosomere 2 in Tcf7l2$^{-/-}$ embryos

To investigate the role of TCF7L2 in thalamic development, we used *Tcf7l2*^{tm1a} mice, which were generated by an insertion of the tm1a(KOMP)Wtsi allele upstream of the critical 6th exon of the *Tcf7l2* gene (Additional file 1: Fig. S1A). The *Tcf7l2*^{tm1a} allele led to the production of truncated *Tcf7l2* mRNA and the lack of TCF7L2 protein, confirmed by immunostaining (Additional file 1: Fig. S1B). The 6th exon is located downstream of the alternative promoter of the *Tcf7l2* gene; therefore, both full-length TCF7L2 and truncated TCF7L2 isoforms [66] were expected to be knocked out. This was further confirmed by Western blot (Additional file 1: Fig. S1C).

To verify whether proliferation and neurogenesis occurred normally within prosomere 2 in *Tcf7l2*$^{-/-}$ mice, we stained brain sections from embryonic day 12.5 mice (E12.5) with antibodies specific for the KI-67 antigen and TUJ1, markers of proliferating progenitors and young postmitotic neurons, respectively. The knockout of *Tcf7l2* did not cause any apparent defects in neurogenesis or morphological impairment in prosomere 2 at this developmental stage (Additional file 1: Fig. S2), consistent with previous results [23].

To determine whether *Tcf7l2* knockout affected anatomical regionalisation in the postmitotic alar plate of prosomere 2 at later developmental stages, we analysed the cytoarchitecture and morphology of this region by Nissl staining of E18.5 brain sections. We identified severe anatomical alterations in habenular and thalamic areas in *Tcf7l2* knockout brains, with knockout thalami appearing underdeveloped and reduced in the radial dimension, with an oval-like shape (Fig. 1A, B). Clear morphological boundaries between the regions of different cell density within the thalamus and habenula were not observed, indicating impairments in

nucleogenesis. Also, the major habenular efferent tract (habenulo-interpeduncular tract alias fasciculus retroflexus [8]) was absent. The boundaries between the thalamus and neighbouring structures (i.e., prethalamus, habenula, and pretectum), which were evident at this age in wild-type (WT) embryos, were not morphologically detected in knockout mice.

Disruption of axonal connections in the thalamus and habenula in Tcf7l2$^{-/-}$ embryos

To observe the formation of axonal connections in the forebrain in E18.5 *Tcf7l2*$^{-/-}$ embryos, we immunostained brain sections with an anti-L1CAM antibody (Fig. 2). This staining revealed several impairments in connectivity in the diencephalon. The bundles of stria medullaris (sm), which include afferent fibers from the basal forebrain and lateral hypothalamus to the habenula, were disorganised and less compact (Fig. 2A'). Although clearly visible, they were hard to distinguish from nearby fascicles, and they lacked the typical arborisation in the habenula. Retinal ganglion cell axons that ran in the optic chiasm followed their normal trajectory along the ventral and superficial boundaries of the thalamus, but their fasciculation and arborisation in the lateral geniculate nucleus (DLG) and pregeniculate nucleus (PG) were severely disturbed (Fig. 2A''). Finally, the nerve fascicles that passed through the striatum, which include thalamocortical axons (TCAs) were thinner and appeared fewer in number (Fig. 1, 2A). Axonal staining was also reduced in the cortical plate of the cerebral cortex (Fig. 2B). To test whether the impairment in fasciculation in the striatum resulted from the lack of TCAs, we traced these axons with the lipophilic tracer DiI. In WT animals, TCAs were well-developed and had already started to invade the cortical subplate (Fig. 2C). In contrast, none of the mutant embryos developed thalamocortical axons that would cross the striatum and reach the cortex. In summary, the

phenotype of *Tcf7l2*$^{-/-}$ embryos suggest that TCF7L2 regulates thalamo-habenular circuit topography.

Perturbances in outer and inner prosomere 2 boundaries in Tcf7l2$^{-/-}$ *embryos*

To investigate the blurring of boundaries between structures within prosomere 2, we analysed the spatial expression of markers that normally delineate prosomere 2 and its subregions in the E18.5 mouse brain. We examined the rostral border of the prosomere 2 region by staining brain sections with an antibody that was specific for TCF7L2 or LacZ, to identify prosomere 2, and co-staining with antibodies that were specific for SIX3 and PAX6, which mark different subdomains in the prethalamus (i.e., the SIX3-positive reticular thalamic nucleus and PAX6-positive zona incerta and pregeniculate nucleus) [67, 68]). In the control condition, the thalamic area was separated from the SIX3-positive region of the prethalamus by a narrow strip of PAX6-expressing cells (Fig. 3A and B). In *Tcf7l2*$^{-/-}$ embryos, the border between the LacZ-stained area of the thalamus and PAX6-positive area was devoid of its characteristic sharpness. Moreover, PAX6-positive cells invaded the thalamus in *Tcf7l2*$^{-/-}$ embryos and the strip of PAX6-positive cells was encroached upon by the SIX3-positive region, which spread into the area of the thalamus.

We analysed the border between the caudal thalamus (TCF7L2-high region) and rTh. In WT embryos, NKX2-2-positive cells created a sharp boundary with the caudal thalamus, distinguished by a high TCF7L2 signal, without mixing between these subdomains (Fig. 3C). In *Tcf7l2*$^{-/-}$ embryos, we observed some intermingling of NKX2-2-positive cells into the caudal thalamus area. We also inspected the boundary between the habenula and the thalamus. In WT embryos, the habenula was easily identified by POU4F1 staining [52], and the differences in cell

densities allowed discernment of the lateral and medial parts sections. In knockout embryos, despite severely reduced number of stained cells in these areas, we observed a clear intermingling of POU4F1-positive cells into the neighbouring thalamic territories (Fig. 3D).

Collectively, our data suggest that TCF7L2 regulates the establishment of anatomical borders between different diencephalic subregions.

Loss of postmitotic subregional patterning in the thalamus and habenula in Tcf7l2$^{-/-}$ embryos

The blurring of anatomical borders suggested that molecular regionalisation within postmitotic prosomere 2 was disrupted. To investigate this phenomenon, we examined the expression of prosomere 2-specific transcription factor genes at two developmental stages: neurogenesis (E12.5) and postmitotic maturation (E18.5). *Gbx2* and *Pou4f1* are the earliest markers of postmitotic neurons in the thalamus and habenula, respectively [52, 69]. To verify whether TCF7L2 is required for the initial acquisition of postmitotic thalamic and habenular identities, we examined the expression of the *Gbx2* gene and POU4F1 protein during neurogenesis (E12.5). Both *Gbx2* mRNA and POU4F1 were detected in the expected areas in both WT and *Tcf7l2*$^{-/-}$ embryos (Fig. 4), demonstrating that TCF7L2 is not involved in the induction of their expression. We also found that *Gbx2*-positive and POU4F1-positive areas expanded extensively into each other's territory, suggesting an early defect in thalamo-habenular boundary formation.

To examine the effect of TCF7L2 deficiency on the thalamic and habenular molecular landscapes at the stage of postmitotic maturation, we analysed the spatial pattern of marker gene expression on E18.5 in different subregions of the thalamus and habenula [24]. Transcription from the *Tcf7l2* locus was not abolished by *Tcf7l2* knockout, as shown by LacZ staining (Fig. 3A, C)

and *in situ* hybridisation (Additional file 1: Fig. S3). However, *Tcf7l2*$^{-/-}$ embryos exhibited a severe reduction of *Gbx2* expression in the thalamus (Fig. 5A). *Gbx2* staining was still present in some periventricular cells but absent in the intermediate and superficial portions of the thalamus. The expression of *Lef1*, *Foxp2*, *Prox1,* and *Rora* was observed in many thalamic nuclei in WT embryos at this age but was virtually absent in the thalamic area in *Tcf7l2* knockouts (Fig. 5A). In the habenula, *Tcf7l2* knockout significantly reduced the number of POU4F1-positive cells on E18.5 (Fig. 3D) and abolished the expression of *Etv1*, *Hopx* (Fig. 5C), and *Lef1* (Fig. 5A) in different habenular subregions, without affecting their expression in the pallium (*Etv1* in the cortex and *Hopx* and *Lef1* in the dentate gyrus of the hippocampus). In contrast, in GABAergic regions in the thalamus, where TCF7L2 is not present or low in the control condition, the expression of regional markers *Nkx2-2* and *Sox14* was preserved in *Tcf7l2* knockouts (Fig. 5B).

Thus, TCF7L2 plays a role in maintaining the expression of thalamic and habenular markers during embryogenesis, even though the induction of at least some of them does not depend on TCF7L2.

Normal acquisition of glutamatergic identity in prosomere 2 in Tcf7l2$^{-/-}$ *embryos*

The loss of postmitotic subregional patterning in prosomere 2 could impair the acquisition of neurotransmitter identity in this region. Habenular and thalamic neurons in rodents, with the exception of GABAergic interneurons that derive from the rTh [25], are glutamatergic and express high levels of a vesicular glutamate transporter, VGLUT2 [70, 71]. To determine whether the thalamus and habenula in *Tcf7l2* knockout embryos adopted proper neurotransmitter fate, we examined the expression patterns of *Vglut2* (*Slc17a6*) and *Gad67*, a marker of GABAergic neurons, in the diencephalon in WT and *Tcf7l2*$^{-/-}$ embryos. *Tcf7l2*$^{-/-}$ embryos exhibited a pattern of

GABAergic (Fig. 6A) and glutamatergic (Fig. 6B) cell distribution that was similar to the WT condition, with predominant *Vglut2* expression in prosomere 2. Thus, TCF7L2 does not appear to be involved in the specification of generic neurotransmitter identity in prosomere 2.

Reduced embryonic thalamus- and habenula-specific gene expression in Tcf7l2$^{-/-}$ mice

We sought to determine how the loss of TCF7L2 affected the postmitotic differentiation program of neurons in prosomere 2. Functional properties of neuron subtypes are not limited to neurotransmitter identities but are shaped by a battery of molecules that regulate cell excitability, morphology and connectivity. We therefore compared the transcriptome of the thalamo-habenular domain between WT and *Tcf7l2*$^{-/-}$ mice by RNA-seq on E18.5. With an absolute $\log_2$ fold-change cutoff of 0.5 and p value for significance of 0.05 we identified 562 differentially expressed genes (DEGs). Among them, 366 were down-regulated, and 196 were up-regulated (Additional file 1: Fig. S4, Additional file 3: Table S1). We analyse the enrichment of gene ontology terms in the affected genes to determine which molecular and cellular functions are regulated by TCF7L2 at this stage.

GO term analysis revealed an overrepresentation of a number of term groups, including (Additional file 2: Table S2; Additional file 4: Table S3): (*i*) development, including neuron differentiation and axon guidance, (*ii*) cell migration/movement, including cell adhesion, (*iii*) cell signalling/signal transducing activity, (i*v*) transcription regulation, (*iv*) calcium homeostasis/binding, and (*iv*) ion transport. Among cell adhesion and axon guidance genes, we identified genes that were specifically expressed in the thalamus and are potentially involved in the segregation of neurons and axon outgrowth in the diencephalon area (Table 1, 2), such as *Epha4*, *Epha8*, *Cdh6*, *Cdh7*, *Cdh8*, and *Cntn6* [72]. Within the calcium homeostasis and ion

transport groups we found an abundance of genes that encode neurotransmitter receptors and transporters, and ion channels that shape the neuron's electrophysiological properties, e.g., *Grik3* (ionotropic glutamate receptor), *Slc6a4* (serotonine transporter), *Kcng4* (potassium voltage-gated channel), and *Chrnb4* (cholinergic receptor).

To determine whether gene expression from the above groups are specifically thalamic or habenular, we examined their spatial expression profiles in the WT brain in the Allen Brain Atlas (ABA) [73]. We found *in situ* hybridisation images for 92 of 140 genes (Additional file 5: Table S4). Among the down-regulated genes that were represented in the ABA, ~80% were specific for prosomere 2 (thalamic - 50%, habenular - 15% thalamic and habenular – 15% (Table 1). In contrast, among the up-regulated genes, less than 20% were prosomere 2-specific (Table 2). The only thalamus-specific transcription factor genes that were up-regulated, *Nkx2-2* and *Sox14*, were specific for the rTh, a region with low and transient *Tcf7l2* expression in postmitotic cells. These results demonstrate that during development TCF7L2 regulates both thalamic and habenular differentiation programs.

Disruption of the prosomere 2-specific network of transcription factors in Tcf7l2$^{-/-}$ mice

Prosomere 2-specific and development-associated transcription factor genes were down-regulated in *Tcf7l2* knockout embryos. We carried out an *in silico* analysis to test the hypothesis that TCF7L2 is a part of a transcription factor network that regulates development-associated genes in the thalamo-habenular region (Additional file 6: Table S5). In evolutionarily conserved non-coding regions (CNRs) within ±10 Kb of the transcription start site, a total of 275 motifs were over-represented in down-regulated genes (cluster 1), and 178 motifs were over-represented in up-regulated genes (cluster 2). Such high numbers of over-represented motifs are characteristic of

developmental and neural genes, which are regulated in a complex manner [74, 75]. The TCF7L2 motif was over-represented in down-regulated genes (cluster 1) but not in up-regulated genes (cluster 2), suggesting that this factor is directly involved in the positive regulation of gene expression in prosomere 2. RORA, NR4A2, and LEF1 motifs were also over-represented in cluster 1 but not in cluster 2, whereas GBX2 and POU4F1 motifs were over-represented in both clusters. This, together with the loss of postmitotic subregional transcription factor expression in prosomere 2 (Fig. 5) suggests that TCF7L2 positively controls the expression of caudal thalamic and habenular genes during postmitotic development directly and by maintaining a network of development-related transcription factors.

Normal anatomy and mildly impaired thalamo-habenular patterning in postnatal Tcf7l2$^{-/-}$ mice

Having shown that TCF7L2 is involved in the regionalisation and expression of postmitotic differentiation genes in prosomere 2 during embryogenesis, we sought to determine whether the continuous presence of TCF7L2 is required to maintain post-developmental molecular anatomy of the thalamo-habenular domain. We generated a mouse model in which *Tcf7l2* was knocked out postnatally, starting from the age of ~2 weeks. This was achieved by sequential crossings of *Tcf7l2*^{tm1a} mice with transgenic animals that expressed flippase (Gt[ROSA]$^{26Sortm1[FLP1]Dym}$) and then with mice that expressed CRE recombinase from the *Cck* promoter. The resulting *Cck*^{Cre}:*Tcf7l2*$^{tm1c/tm1c}$ mice had the 6th *Tcf7l2* exon removed conditionally, which starts perinatally in the thalamus. TCF7L2 was absent in adult *Cck*^{Cre}:*Tcf7l2*$^{tm1c/tm1c}$ animals in most thalamic nuclei (Fig. 7A), but was maintained in the habenula (Fig. 7B).

The gross anatomy of the thalamus was not visibly altered by the postnatal knockout of *Tcf7l2*, and *Vglut2* was expressed normally on P60 (Fig. 8A), confirming that TCF7L2 does not

regulate the generic glutamatergic identity of prosomere 2. We then analysed the spatial expression of thalamic subregional markers in adult mice (Fig. 8B). In WT mice, *Gbx2* was expressed mainly in the medial part of the thalamus, *Rora* was expressed throughout the thalamus, including its lateral part, and *Prox1* was expressed in the anterior part of the thalamus. The expression of *Gbx2* and *Lef1* was not visibly altered in *Cck*^{Cre}:*Tcf7l2*$^{tm1c/tm1c}$ mice. The signals from *Rora* mRNAs was clearly weaker in the medial part of the thalamus. The expression of *Prox1* was also markedly decreased in the thalamus, while it remained high in the hippocampus. Thus, TCF7L2 is continuously required in adults to maintain proper regional patterning in the thalamus. We also analysed the expression of the habenular markers *Hopx* and POU4F1, and observed that both were maintained in *Cck*^{Cre}:*Tcf7l2*$^{tm1c/tm1c}$ mice, as well as TCF7L2 (Fig. 8C).

Impaired expression of synaptic genes in adult Cck^{Cre}:Tcf7l2$^{tm1c/tm1c}$ mice

To investigate whether TCF7L2 influences stability of the transcriptional program that operates in differentiated neurons in the thalamus and habenula in adults we compared global gene expression profiles in the thalamo-habenular region between *Cck*^{Cre}:*Tcf7l2*$^{tm1c/tm1c}$ and WT mice on P60, using RNA-seq. To identify differentially expressed genes, we set the same cutoffs used in our analysis of E18.5 mice, and identified a total of 552 genes. Of these differentially expressed genes, 298 were down-regulated, and 254 were up-regulated (Additional file 1: Fig. S4, Additional file 7: Table S6). We performed GO analysis to uncover molecular or cellular functions that might be affected by TCF7L2 deficiency in the prosomere 2 region in adults.

The differentially expressed genes in *Cck*^{Cre}:*Tcf7l2*$^{tm1c/tm1c}$ mice on P60 were significantly enriched mainly with terms that clustered into a group of synaptic genes (Additional file 2: Table S7, Additional file 8: Table S8): (*i*) signal transduction, including G-protein-coupled signalling,

(*ii*) synapse organisation, including proteins that are involved in vesicle regulation, and (*iii*) ion homeostasis and transport, including voltage-gated channels. Among these genes were several sodium, potassium and calcium channel genes (e.g., *Scn4b*, *Kcnip2*, *Kcnc2*, *Trpv6*, *Cacna1g*, and *Cacna2d4*) and several neurotransmitter receptor genes (e.g., *Glra1, Glra2,* and *Htr1b*) (Table 3, 4). We then examined spatial expression profiles of the identified genes in this cluster on *in situ* hybridisation images of P56 mouse brain sections in the ABA to determine whether these genes are specific for thalamic regions (Additional file 9: Table S9). We found *in situ* hybridisation images for 61 of 65 genes. ~45% of the down-regulated genes that were represented in the ABA were expressed specifically in the thalamus or thalamus and habenula, and 14% were expressed exclusively in parts of the brain other that the thalamus (Table 3). Conversely, only 8% of the up-regulated synaptic genes were thalamus-specific, whereas 46% of them were expressed specifically in other parts of the brain (Table 4). Thus, TCF7L2 maintains the expression of region-specific synaptic genes in the thalamo-habenular region in the mature brain.

Discussion

The involvement of Wnt signalling and individual Wnt pathway effectors, such as the LEF1/TCF transcription factors, in brain development has rarely been addressed beyond neural tube patterning and neurogenesis. The transcription factor TCF7L2 is highly expressed during the maturation, and in the adult neurons of the thalamo-habenular region. We have shown that TCF7L2 is involved in nucleogenesis and molecular regionalisation both in the thalamus and habenula, as well as proper innervation of prosomere 2 structures. We have also demonstrated that TCF7L2 is required for the induction and adult maintenance of the expression of thalamus- and habenula-specific genes that encode proteins involved in synaptic transmission regulation.

TCF7L2 regulates a transcription factor network during postmitotic development of prosomere 2

TCF7L2 is the only developmentally regulated transcription factor known to be expressed throughout prosomere 2. *Gbx2* is expressed in newborn neurons in the thalamus, and *Pou4f1* is expressed in the habenula. *Tcf7l2* knockout has much more severe impact on the development of the prosomere 2 region than knockout of either the pan-thalamic marker *Gbx2* or the pan-habenular *Pou4f1*, or knockouts of subregional transcription factor genes *Foxp2*, *Rora*, and *Nr4a2*. Knockout of *Gbx2* revealed it was also critical for the establishment of thalamic identity, but the lateral and medial geniculate nuclei appeared to develop normally, and habenular identity was unaffected in this mutant [76]. In *Pou4f1* knockout mice, the thalamus developed normally, and only the identity of the habenula was affected [52]. Mice with either *Foxp2* or *Rora* knockouts exhibited defects restricted to subregions of the thalamus. *Nr4a2* knockout affected the expression of *Etv1* and several other POU4F1-dependent genes, but did

not result in any anatomical abnormalities in the habenula. In contrast, the identities of prosomere 2 neurons were completely disrupted in *Tcf7l2*$^{-/-}$ mice.

Expression of *Gbx2* and *Pou4f1* was observed in *Tcf7l2*$^{-/-}$ mice on E12.5, indicating that TCF7L2 is not required for the induction of these genes in young postmitotic cells. The signals that instruct cells to express these markers are only partly understood. The expression of *Gbx2* in the thalamic primordium is induced by Shh signal molecules that are secreted by ZLI [76, 77], and by canonical Wnt signalling [38], but this effect of Wnt pathway activity is apparently not mediated by TCF7L2. However, on E18.5, *Gbx2* and *Pou4f1* expression was very substantially reduced in the thalamus or habenula in *Tcf7l2*$^{-/-}$ mice, respectively, and was detected only in the periventricular region, where the youngest thalamic and habenular neurons are present. Thus, although the induction of these early prosomere 2 markers occurs independently of TCF7L2, thalamic *Gbx2* and habenular *Pou4f1* expression does depend on TCF7L2 at later stages.

The expression of other thalamic or habenular-specific transcription factors - *Rora*, *Prox1*, *Foxp2*, *Nr4a2*, *Etv1,* and *Hopx* - were also observed to be dependent on TCF7L2, both during development and in adults. This is consistent with our previous results showing that TCF7L2 regulated the promoters of *Rora, Foxp2, Nr4a2* and *Etv1,* as well as *Gbx2* and *Pou4f1* [24]. On the other hand, *Foxp2* and *Rora* were also down-regulated in *Gbx2*$^{-/-}$ embryos, and *Nr4a2* and *Etv1* expression decreased in *Pou4f1*$^{-/-}$ embryos. Taken together, these results imply the existence of a hierarchy of regional transcription factors involved in postmitotic differentiation in prosomere 2. We further postulate that these transcription factors together create a network that coordinates subregion-specific maturation, by regulating the expression of cell adhesion/guidance and neural excitability genes. This is corroborated by over-representation of GBX2, POU4F1, RORA, PROX1, FOXP2, and NR4A2 binding motifs, as well as the

TCF7L2 motif, within putative regulatory regions of genes that were differentially expressed in prosomere 2 in *Tcf7l2*$^{-/-}$ mice. Cooperation between TCF7L2 and subregional transcription factors could explain why TCF7L2 regulates both common and subregion-specific genes in prosomere 2. Such hierarchical and combinatorial regulation of neuron subtype selection has also been described in *Caenorhabditis elegans* [78] and in regulation of the specification and maintenance of serotonergic neurons by the transcription factor PET-1 in mice [79].

TCF7L2 coordinates the development of prosomere 2 boundaries and connections

On E18.5, the diencephalon is parcelled into discrete nuclei: In *Tcf7l2*$^{-/-}$ mice we observed a lack of well-defined inter-prosomeric and intra-thalamic boundaries. These morphological aberrations were present not only in the caudal thalamus, but also in the rTh, habenula, and prethalamus, and cells from these domains invaded the putative caudal thalamic region. A similar lack of clearly defined borders within prosomere 2 and between the thalamus and prethalamus has been observed in *Gbx2* knockout mice induced on E10.5 [80]. The thalamo-habenular region also had a similar elongated shape, as seen in *Tcf7l2*$^{-/-}$ mice. A decrease in the expression of prosomere 2-specific adhesion genes, such as *Cdh6*, *Cdh8*, and *Cntn6*, may be the direct cause of the partial loss of anatomical boundaries in *Tcf7l2*$^{-/-}$ embryos as, for example, *Cdh6* transcripts are localised in the thalamus and at the borders with the rTh, habenula, and pretectum. These genes were down-regulated in our mutant mice, as assessed by RNA-seq on E18.5. The dorsal border of *Cdh6* expression was shown to be disrupted in the thalamus in *Gbx2* mutant embryos on E14.5 [61], therefore it is likely the changes that occur in *Tcf7l2*$^{-/-}$ mice were at least partially mediated by GBX2. The partial loss of interprosomeric borders was also seen in *Pax6*$^{Sey/Sey}$ mice [67]. As

revealed in the present study, this could be explained by the loss of *Tcf7l2* expression, observed in the diencephalon of *Pax6*$^{Sey/Sey}$ mice [81].

In *Tcf7l2*$^{-/-}$ mice, thalamocortical axons do not grow toward the cortex, and some do not cross the internal capsule. Decreases in the expression of cell adhesion genes and genes that encode axon-navigating ROBO3 and Ephrins, which we observed in this study, may underlie these defects. Recent research has shown that thalamic cells in *Tcf7l2*$^{-/-}$ mice do not respond to *Slit2*-repelling cues from the hypothalamus because of disturbances in the expression of ROBO1 and ROBO2 guidance receptors [23]. This phenotype also resembles the phenotype in *Gbx2* knockout mice, which exhibited abnormal expression of the same guidance receptors [59]. Others have argued [23] that TCF7L2 regulates the pathfinding of thalamocortical axons in a GBX2-independent manner, because essentially normal *Gbx2* expression was observed in *Tcf7l2*$^{-/-}$ mice on E12.5 [23]. Here, we have found that *Gbx2* expression was not maintained in the thalamus in *Tcf7l2*$^{-/-}$ mice at later developmental stages, therefore GBX2 could, in fact, contribute to this phenotype. Less severe impairments in the establishment of thalamocortical connections were reported in *Foxp2* knockout mice [64] and *Rora* knockout mice [63], and these genes were down-regulated in both *Tcf7l2* knockout and *Gbx2* knockout mice. Therefore, the FOXP2 and RORA transcription factors could also partially mediate the effects of TCF7L2 and GBX2 on the growth of thalamic axons. Apart from thalamocortical axons, *Tcf7l2*$^{-/-}$ mice lack habenulo-interpeduncular tracts. This phenotype is unlikely to be mediated by the habenular transcription factors POU4F1 and NR4A2 because these axon bundles are present in *Pou4f1* and *Nr4a2* knockout embryos [52, 62].

TCF7L2 maintains phenotypic electrophysiological identities in the thalamus and habenula

Excitability and synaptic transmission parameters are specific to different classes of neurons and together ensure the proper functioning of neural circuits in the brain. Many genes that were down-regulated in mice with the complete or post-developmental knockout of *Tcf7l2* encode either thalamus- or habenula-specific neurotransmitter receptors or transporters, voltage-gated ion channels, and other proteins that are involved in neural signal transmission, which is in agreement with our previous *in silico* predictions [82]. For example, habenular-expressed *Chrnb4* and *Slc5a7,* which encode components of cholinergic signalling and are involved in depressive behaviour [83], and the *Kcng4* gene, which encodes a modulatory subunit of K_{V2} channels [84], were down-regulated in *Tcf7l2*$^{-/-}$ embryos. A thalamus-specific synaptic gene, *Slc6a4,* was down-regulated in *Tcf7l2*$^{-/-}$ embryos. *Slc6a4* encodes the serotonin transporter, which is transiently expressed during development [85] and is involved in the development of thalamocortical connectivity [86, 87]. Variants of *SLC6A4* are associated with autism spectrum disorder [88], and the transient pharmacological inhibition of *Slc6a4* during early development produced abnormal emotional behaviours in adult mice [89]. *Prkcd* and *Prkch* gene expression was affected by the knockout of *Tcf7l2* in both embryonic and adult thalamus. These genes encode kinases from the protein kinase C family that might regulate $GABA_A$ receptor function [90]. *Cacna1g,* which is expressed both in the thalamus and habenula, was down-regulated in adult knockout mice. *Cacna1g* encodes a subunit of T-type calcium channels that mediate the specific bimodal firing of thalamic neurons [91]. Our group previously showed that *Cacna1g* is a direct target of LEF1/TCF and β-catenin in the adult thalamus [20]. Altogether, these results demonstrate that TCF7L2 regulates multiple regional electrophysiological features in prosomere 2 derivatives and implies a

crucial role for TCF7L2 in shaping and maintaining the electrophysiological properties of neurons in the thalamus and habenula.

TCF7L2 is a terminal selector of prosomere 2 fates

Tcf7l2 is induced in prosomere 2 during neurogenesis, is expressed throughout the life of postmitotic neurons, controls the morphological and electrophysiological maturation of neurons, and maintains molecular identities in this area. This implies that TCF7L2 fulfils the criteria of a terminal selector. Terminal selectors were described and characterised in *C. elegans* [92]. There are a limited number of examples of such regulators operating both during development and in mature cells in vertebrate brains. Most of these selectors are specific to different classes of aminergic neurons: NR4A2 and PITX in midbrain dopaminergic neurons [93], ETV1 in dopaminergic neurons in the olfactory bulbs [94], ISL1 and LHX7 in forebrain cholinergic neurons [95], and PET1 in serotonergic neurons [79]. POU4F1 was recently identified as a selector of glutamatergic neurons in the medial habenula, where it maintains the expression of the glutamate transporter gene *Vglut1* (*Slc17a7*) [62]. Unlike the aforementioned terminal selectors, TCF7L2 does not control region-specific neurotransmitter identity, which is defined in prosomere 2 by the expression of *Vglut2*, as this generic neurotransmitter identity was maintained in both *Tcf7l2*$^{-/-}$ embryos and *Cck*^{Cre}:*Tcf7l2*$^{tm1c/tm1c}$ adult mice. Therefore, the glutamatergic fate of prosomere 2 neurons is likely already determined in progenitors or early postmitotic cells.

Conclusion

Here, we reveal that the transcription factor TCF7L2 is involved in subregional patterning and the adult maintenance of terminal identities in the thalamus and habenula of the vertebrate forebrain, in addition to cell segregation and axon guidance during development. TCF7L2 is one of a few examples of a terminal selector in the vertebrate brain. TCF7L2, unlike other vertebrate selectors, does not regulate generic thalamo-habenular neurotransmitter identity, rather, our results suggest that its continuous expression in adults is involved in maintaining multiple distinct electrophysiological properties of neurons in this area. TCF7L2 regulates the expression of a number of subregional transcription factors that may cooperate with it to regulate gene expression differentially in discrete regions of prosomere 2. Deciphering the precise regulatory codes for specific electrophysiological identities in prosomere 2 subregions will require further investigation.

Materials and Methods

Animals. The study used C57BL/6NTac-*Tcf7l2*^{tm1a}(EUCOMM)Wtsi/WtsiIeg (*Tcf7l2*^{tm1a}) mouse (*Mus musculus*) strain, in which a trap cassette with the LacZ and neoR elements, each with the SV40 termination/polyadenylation sequences, was inserted upstream of the critical exon 6 of the *Tcf7l2* gene. The mice were obtained from the European Mouse Mutant Archive (EMMA) repository and provided by the Wellcome Trust Sanger Institute (WTSI) [96]. The homozygous *Tcf7l2*$^{tm1a/tm1a}$ allele is lethal perinatally; thus, the mice were kept as *Tcf7l2*$^{+/tm1a}$ heterozygotes that were crossed with C57BL/6J mice. For the experimental procedures, *Tcf7l2*$^{+/tm1a}$ mice were mated, and their offspring were collected on E12.5, E18.5 or P0. Homozygous *Tcf7l2*$^{tm1a/tm1a}$ and WT *Tcf7l2*$^{+/+}$ mice were selected by polymerase chain reaction-based (PCR) genotyping with specific primers (Additional file 2: Table S10). To remove the trap cassette from the *Tcf7l2-tm1a* allele, *Tcf7l2*$^{tm1a/+}$ mice were crossed with flippase-expressing B6.129S4-Gt(ROSA)26Sor$^{tm1(FLP1)Dym}$/RainJ mice (JAX stock #009086; [97]). In the resulting *Tcf7l2-tm1c* allele, exon 6 of the *Tcf7l2* gene was flanked by loxP sites. *Tcf7l2*$^{tm1c/tm1c}$ mice were then crossed with *Cck*$^{tm1.1(cre)Zjh}$/J (*Cck*^{Cre}:*Tcf7l2*$^{+/+}$, JAX stock #012706; [98]), which express Cre recombinase from the *Cck* promoter, to conditionally delete exon 6. In *Cck*^{Cre}:*Tcf7l2*$^{tm1c/tm1c}$ mice, the knockout of *Tcf7l2* is induced in the thalamic area between E18.5 and P14 [99]. Genotyping was performed using PCR with allele-specific primers (Additional file 2: Table S10). The mice were maintained on a 12 h/12 h light/dark cycle with *ad libitum* access to food and water. All of the experimental procedures were conducted in compliance with the current normative standards of the European Community (86/609/EEC) and Polish Government (Dz.U. 2015 poz. 266).

Brain fixation. *Tcf7l2*$^{tm1a/tm1a}$ and *Tcf7l2*$^{+/+}$ mice were collected on E12.5, E18.5 or P0. Noon on the day of appearance of the vaginal plug was considered E0.5. Timed-pregnant dams were sacrificed by cervical dislocation. The embryos were immediately removed by caesarean section and decapitated. E18.5 and P0 brains were immediately dissected out and immersion-fixed overnight in freshly made 4% paraformaldehyde (PFA; catalog no. P6148, Sigma-Aldrich) in 0.1 M phosphate-buffered saline (PBS; pH 7.4; catalog no. PBS404, BioShop) at 4ºC. E12.5 heads were fixed whole. *Cck*^{Cre}:*Tcf7l2*$^{tm1c/tm1c}$ and *Cck*^{Cre}:*Tcf7l2*$^{+/+}$ mice were sacrificed on P55-P75 by pentobarbital sedation and perfusion with ice-cold PBS and 4% PFA solutions. The brains were dissected out and immersion-fixed overnight in 4% PFA. For cryostat sections, the brains were washed 6 times with fresh 0.1 M PBS over the course of 48 h at 4ºC and then transferred to 15% sucrose in 0.1 M PBS for 24 h at 4ºC and into 30% sucrose in 0.1 M PBS at 4ºC until they sank. E12.5 and E18.5 brains were then placed for 1 h in 10% gelatine/10% sucrose solution in 0.1 M PBS at 37°C, transferred to freezing molds, fully covered with 10% gelatine/10% sucrose solution, and kept at 4ºC until they solidified [100, 101]. Postnatal brains were transferred from sucrose solution to O.C.T (catalog no. 4583, Sakura Tissue-Tek) for 15 min with gentle mixing. Then, the gelatine blocks and O.C.T-covered tissue were frozen for 1 min in isopentane that was cooled to -60ºC in dry ice and stored at -80ºC until cryosectioning. For E12.5 embryos, whole heads were fixed and further processed and frozen the same way as E18.5 embryos. Sections (20 µm thick for embryos, 50 µm thick for postnatal brains) were obtained in either the coronal or sagittal planes using a Leica CM1860 cryostat. Embryonic tissue was mounted as six parallel series on Superfrost-plus slides (catalog no. J1800AMNZ, Menzel-Gläser). These sections were stored at -80ºC until they were further processed for *in situ* hybridisation or immunostaining. Postnatal tissue was collected as free-floating sections into an anti-freeze solution (30%

sucrose/30% glycerol in 1x PBS) and stored at -20ºC. Free floating sections were used in immunohistochemistry, and the sections were mounted onto Superfrost-plus slides for *in situ* hybridisation. For DiI axon tracing, E18.5 immersion-fixed brains were kept in 4% PFA in 0.1 M PBS at 4ºC.

In situ hybridisation. The hybridisation was performed using digoxigenin-UTP-labelled antisense riboprobes. Sense and antisense digoxigenin-labelled RNA probes for mouse were synthesized with the DIG RNA labelling Kit (catalog no. 11175025910, Roche) according to the manufacturer's instructions. Plasmids for synthesis of *Foxp2*, *Gad67*, *Gbx2*, *Lef1*, *Prox1, Rora Tcf7l2*, *Tfap2b* and *Slc17a6* probes come from the collection of José Luis Ferran (Additional file 2: Table S10). Hopx plasmid was a gift from Peter Mombaerts from the Max Planck Research Unit for Neurogenetics (Addgene plasmid #74347, [102]). *Etv1* plasmid was a gift from James Li from the Department of Genetics and Developmental Biology, University of Connecticut Health Center, Farmington, CT, USA [103]. *Nkx2-2* and *Sox14* plasmids were a gift from Seth Blackshaw from the Johns Hopkins University School of Medicine, Baltimore, MD, USA [104]. *Pax6* plasmid was a gift from David Price from the Centre for Integrative Physiology, University of Edinburgh, UK [105]. The *in situ* hybridisation of cryosections was performed as described elsewhere [100, 106]. In short, frozen brain sections were washed in 0.1 M PBS, fixed with 4% PFA in 0.1 M PBS, acetylated, permeabilized in 1% Triton X-100 in 0.1 M PBS, blocked for 2 h with prehybridisation buffer, and then incubated overnight at 68ºC with 1.0 µg/ml labelled probe. The sections were then washed, blocked in 10% normal sheep serum with 10% lysine in appropriate pH 7.5 buffer, and incubated overnight at room temperature in a solution that contained anti-digoxigenin alkaline phosphatase-coupled Fab fragments of antibodies (1:3500;

catalog no. 11093274910, Roche). Nitroblue tetrazolium/5-bromo-4-chloro-3-indolyl phosphate (NBT/BCIP; catalog no. 11383213001 and 11383221001, respectively, Roche) solution was then used as the chromogenic substrate for the final alkaline phosphatase reaction that was performed in pH 9.5 buffer. After stopping the chromogenic reaction, the sections were dried, washed twice for 5 min in xylene, and immediately mounted using EuKitt (catalog no. 03989, Sigma-Aldrich). The sections were visualized under a Nikon Eclipse Ni-U (Image-Pro Plus 7.0 software) fluorescent microscope (brightfield). No specific signal was obtained with sense probes (data not shown). The images were prepared using GIMP 2.8.14, Fiji v1.52 and CorelDraw X7.

Fluorescent immunohistochemistry. Frozen coronal and sagittal brain sections were washed three times in 0.1 M PBS with 0.2% Triton X-100 (PBST) and blocked with 5% normal donkey serum with 0.3 M glycine in 0.1 M PBS for 1 h. The slides were then incubated with primary antibodies mixed in 1% normal donkey serum in 0.1 M PBS overnight at 4°C. Antibodies against TCF7L2 (1:500; catalog no. 2569, Cell Signaling), LacZ (1:100; catalog no. AB986, Merck Millipore), L1CAM (1:500; catalog no. MAB5272, Merck Millipore), PAX6 (1:100; catalog no. PRB-278P, Biolegend), SIX3 (1:100; catalog no. 200-201-A26S, Rockland), KI-67 (1:100; catalog no. AB9260, Merck Millipore), TUJ1 (1:65; catalog no. MAB1637, Merck Millipore), NKX2-2 (1:50; catalog no. 74.5A5, DSHB), POU4F1 (1:300; [107]) were used. The sections were then washed three times with PBST and incubated for 1 h with appropriate secondary antibody conjugated with Alexa Fluor 488 or 594 (1:500; catalog no. A-21202, A-21207, and A-11076, ThermoFisher Scientific). The slides were then additionally stained with Hoechst 33342 (1:10000; catalog no. 62249, ThermoFisher Scientific), washed three times, and mounted with Vectashield Antifade Mounting Medium (catalog no. H1000, Vector Laboratories). Specimens were analysed

under a Nikon Eclipse Ni-U (Image-Pro Plus 7.0 software) microscope. The images were prepared using GIMP 2.8.14, Fiji v1.52 and CorelDraw X7.

DAB immunohistochemistry. Free floating sections were washed three times in PBST, incubated in 0.3% H_2O_2 in PBST for 10 min and blocked with 3% normal goat serum in PBST for 1 h. The sections were then incubated with primary antibodies against TCF7L2 (1:1000; catalog no. 2569, Cell Signaling) or POU4F1 (1:600; [107]) in 1% normal goat serum in PBST overnight at 4ºC. The sections were then incubated for 1 h with biotynylated goat anti-rabbit antibody in 1% normal goat serum in PBST (catalog no. BA-1000, Vector Laboratories), then incubated in Vectastain ABC reagent for 1 h (catalog no. PK-6100, Vector Laboratories). Staining was developed using 0,05% 3,3'-diaminobenzidine in PBST (DAB, catalog no. D12384, Sigma-Aldrich) as a chromogen substrate and H_2O_2 to the final concentration of 0.01%. The reaction was stopped as soon as a brown precipitate appeared. The sections were washed, mounted onto Superfrost plus slides, dried, washed twice for 5 min in xylene, and immediately mounted using EuKitt (catalog no. 03989, Sigma-Aldrich). The sections were visualized under a Nikon Eclipse Ni-U (Image-Pro Plus 7.0 software) fluorescent microscope (brightfield). The images were prepared using GIMP 2.8.14, Fiji v1.52 and CorelDraw X7.

DiI axon tracing. To label thalamocortical axon tracts, the paraformaldehyde-fixed brains were separated into hemispheres by cutting along the midline. Small DiI (1,1'-dioctadecyl-3,3,3',3'-tetramethylindocarbocyanine perchlorate) crystals (catalog no. D-3911, ThermoFisher Scientific) were placed in the thalamic hemispheres, roughly 1 mm below the centre of their exposed surfaces. The tissue was then incubated in 4% PFA at 37ºC for 18-21 days to allow diffusion of

the lipophilic tracers along the axons. The hemispheres were then embedded in 5% low-melting-point agarose (catalog no. AGA101, BioShop) and cut into 100 μm thick sections in a vibratome in the coronal plane. Free-floating sections were counterstained with Hoechst (1:10000; catalog no. 62249, ThermoFisher Scientific), mounted onto poly-L-lysine-coated glass slides (catalog no. J2800AMNZ, Menzel-Gläser), and secured under a coverslip with Vectashield Antifade Mounting Medium (catalog no. H-1000, Vector Laboratories). The sections were visualized under a Nikon Eclipse Ni-U (Image-Pro Plus 7.0 software) fluorescent microscope on the same day the tissue was cut and mounted. The images were prepared using GIMP 2.8.14, Fiji v1.52 and CorelDraw X7.

Nissl staining. Brain sections from the control and experimental groups were fixed in 4% PFA in 0.1 M PBS for 20 min and washed for 5 min in 0.1 M PBS alone. The slices were dehydrated by immersing in a series of ethanol (3 min each at 50%, 70%, 95%, and 99.8%). The slices were then cleared in xylene for 5 min, washed in 100% ethanol, and rehydrated in a series of ethanol (3 min each at 95%, 70%, and 50%). Brain sections were rinsed in 0.01 M PBS and stained with 0.13% (w/v) Cresyl violet solution (catalog no. CS202101, Millipore) for 4 min, rinsed with distilled water, and dehydrated as described above. The slices were again cleared in xylene for 5 min and mounted on glass coverslips with DPX (catalog no. 1019790500, Merck). Images were captured under a Nikon Eclipse Ni-U (Image-Pro Plus 7.0 software) microscope. The images were prepared using GIMP 2.8.14, Fiji v1.52 and CorelDraw X7.

Western blot analysis. Protein extracts from the thalamus were homogenized in ice-cold RIPA buffer that contained 50 mM Tris, pH 7.5 (catalog no. T1503, Sigma-Aldrich), 150 mM NaCl

(catalog no. SOD001, BioShop), 1 mM ethylenediaminetetraacetic acid (catalog no. EDT001, BioShop), 1% NP40 (catalog no. I8896, Sigma-Aldrich), 0.1% sodium dodecyl sulfate (SDS; catalog no. 75746, Sigma-Aldrich), 0.5% sodium deoxycholate (catalog no. 30970, Sigma-Aldrich), 1 mM NaF (catalog no. S7920, Sigma-Aldrich), inhibitor of phosphatases PhosSTOP (catalog no. 04906845001, Roche), and inhibitor of proteinases complete ULTRA Tablets (catalog no. 05892791001, Roche). The protein concentrations were determined using the Bio-Rad protein assay (catalog no. 5000006, Bio-Rad Laboratories) according to the manufacturer's instructions. Clarified protein homogenate (50 µg) was loaded on 10% SDS-polyacrylamide gels. The separated proteins were transferred to Immun-Blot PVDF membranes (catalog no. 1620177, Bio-Rad Laboratories), which were then blotted using appropriate antibodies: anti-TCF7L2 (catalog no. 2569, Cell Signaling) and anti-β-actin (catalog no. A3854, Sigma-Aldrich). The proteins were visualized with peroxidase substrate for enhanced chemiluminescence (100 mM Tris [pH 8.5], 1.25 mM 3-aminophthalhydrazide [catalog no. 123072, Sigma-Aldrich], and 200 µM coumaric acid [catalog no. C9008, Sigma-Aldrich]). Images were captured using Amersham Imager 600 RGB (General Electric).

RNA isolation. *Tcf7l2*$^{tm1a/tm1a}$ and WT littermate mice were collected on E18.5. Embryos were removed by caesarean section and decapitated. *Cck*^{Cre}*:Tcf7l2*$^{tm1c/tm1c}$ and *Cck*^{Cre}*:Tcf7l2*$^{+/+}$ were collected on P60. Adults were sacrificed by cervical dislocation and decapitated. The thalami together with the habenula (prosomere 2) were immediately dissected-out from the brains and frozen in liquid nitrogen. RNA was extracted using QIAzol (catalog no. 79306, Qiagen) and the RNeasyMini Kit (catalog no. 74106, Qiagen) according to the manufacturer's instructions.

RNA-seq analysis. The quality of RNA was verified in Bioanalyzer (Aligent). RNA samples were sequenced on the same run of Illumina HiSeq2500 (average of ~22-33 million 50-nucleotide single-end reads). The reads were aligned to the mouse genome mm10 using TopHat [108]. The transcripts were assembled, and counts of sequencing reads were generated using HTSeq [109]. Normalized counts in reads per kilobase million (RPKM) were calculated with DESeq2 [110]. The genes with expression measurements of RPKM = 0 in at least one sample were considered not-expressed in prosomere 2. For the rest of the genes, fold-changes between mean values for WT and knockout were calculated, and two-tailed Student's *t*-test was performed to assess the significance of the difference. Genes with an average fold-change ≥ 1.5 in *Tcf7l2*$^{-/-}$ embryos compared with WT and with a value of $p < 0.05$ for the difference were considered differentially expressed genes (DEGs) [111].

Functional enrichment analysis. Gene ontology (GO) enrichment for the DEGs was performed using the GOrilla open-access online tool (http://cbl-gorilla.cs.technion.ac.il) [112]. Two unranked lists of genes (one target list [111] and one universal list [111]) were used for this analysis, assuming a hypergeometric distribution of the unranked genes. As the universal set, we used all of the genes with expression measurements of RPKM > 0 in all of the samples. GO-Term enrichments were tested using Fisher's exact test, and Bonferroni corrected values < 0.05 were considered significant. To obtain a clear view of the enriched groups of genes, we then removed redundant terms and too-general terms (e.g., multicellular organismal process), and the remaining terms were grouped hierarchically.

Spatial expression of GO enriched genes. We assessed the spatial localisation of transcription factor and guidance/adhesion molecule DEGs by visually inspecting the *in situ* hybridisation signals in the Developing Mouse Brain (E18.5) from the Allen Developing Mouse Brain Atlas (ABA) (http://developingmouse.brain-map.org/; accessed September 2018) [113]. The genes were then clustered into the following groups: thalamic; habenular, thalamo-habenular; extra-prosomeric (i.e., expressed in other parts of the brain than prosomere 2); and nonspecific (i.e., their expression was ubiquitous in the brain or no expression signal was observed in the atlas). A gene was considered thalamic or habenular when its expression level was apparently higher in this part of the brain than generally in the brain. The resulting list was manually curated to reject the data that originated from staining artefacts or very low expression levels.

Motif enrichment analysis in putative regulatory elements in ±10 Kb regions that flank transcription start sites. We used Nencki Genomics Database (NGD) v. 79_1 [114] to map genes to their putative regulatory regions within ±10 Kb of the genomic DNA sequence that flanked the transcription start site. We chose human-mouse CNRs [115] as the putative regulatory regions. In these regions, we considered instances of all transcription factor binding sites (position weight matrices [PWMs]) that were available in NGD v79_1, representing 684 distinct transcription factors [116], as potential binding sites. As the universal set, we used all genes with both expression measurements of RPKM > 0 and at least one CNR. For Fisher's exact test, each instance of a motif was labelled with the names of its associated transcription factors. Fisher's test *p* values were Bonferroni corrected (i.e., multiplied by a factor of 684 [the number of hypotheses tested]).

Data availability

The RNA-seq raw FASTQ files are in the process of uploading at the EMBL-EBI data repository - ArrayExpress. The EMAT number will be provided as soon as the datasets are accepted.

Competing interests

No competing interests declared.

Funding

This research was supported by the Polish National Science Centre [2011/03/B/NZ3/04480 and 2015/19/B/NZ3/02949 to MBW]. AN and KK were additionally supported by the Polish National Science Centre [2015/19/B/NZ4/03571], JLF and AT were supported and by the Seneca Foundation, Comunidad de Murcia [19904/GERM/1 to JLF].

Author contribution

ML, AN, MBW designed the study. ML managed mice colony. ML, KK and TZ genotyped the transgenic animals. ML and TZ prepared brain tissue sections. ML, KK and TZ performed *in situ* hybridisation (ISH). AT and JLF provided ISH methodology and majority of ISH probes. ML performed DAB and fluorescent immunohistochemical stainings and DiI axon tracing. TZ and KK performed Nissl staining. ML, KK and TZ captured microscopy images. KK performed Western blotting. CC analysed the raw RNA-seq data. MD, CC and MBW performed bioinformatics analysis. ML, KK, TZ, JLF, AN, MBW analysed and interpreted the results. ML, CC and MBW prepared figures and tables. ML, KK, MD, CC, AT, AN, MBW participated in drafting the

manuscript. ML, JLF, AN, MBW participated in the initial reviewing and editing the manuscript. MBW conceived the study and supervised the project.

Acknowledgements

We thank the Genomics Core Facility at the Centre of Genomic Regulation (CRG, Spain) for providing next-generation sequencing services. We gratefully acknowledge M. Irimia from CRG, K. Misztal from the International Institute of Molecular and Cell Biology (Poland), K. Debski from the Nencki Institute of Experimental Biology (Poland), and L. Szewczyk in our Laboratory for help with the RNA-seq analysis. We thank K. Brzozowska in our Laboratory for the initial management of the mice colony. A part of genotyping was performed at the Laboratory of Animal Models facility at the Nencki Institute of Experimental Biology. We thank Michael Arends for proofreading and Guy Riddihough for the help with editing of the manuscript.

References

1. Ferran JL. Architect genes of the brain: A look at brain evolution through genoarchitecture. Mètode Science Studies Journal. 2017;7:17-23.
2. Puelles L, Harrison M, Paxinos G, Watson C. A developmental ontology for the mammalian brain based on the prosomeric model. Trends Neurosci. 2013;36(10):570-8.
3. Sherman SM. Functioning of Circuits Connecting Thalamus and Cortex. Compr Physiol. 2017;7(2):713-39.
4. Lien AD, Scanziani M. Cortical direction selectivity emerges at convergence of thalamic synapses. Nature. 2018;558(7708):80-6.
5. Ribary U. Dynamics of thalamo-cortical network oscillations and human perception. Prog Brain Res. 2005;150:127-42.
6. Hikosaka O. The habenula: from stress evasion to value-based decision-making. Nat Rev Neurosci. 2010;11(7):503-13.
7. Benekareddy M, Stachniak TJ, Bruns A, Knoflach F, von Kienlin M, Künnecke B, et al. Identification of a Corticohabenular Circuit Regulating Socially Directed Behavior. Biol Psychiatry. 2018;83(7):607-17.
8. Fakhoury M. The habenula in psychiatric disorders: More than three decades of translational investigation. Neurosci Biobehav Rev. 2017;83:721-35.
9. Kobayashi Y, Sano Y, Vannoni E, Goto H, Suzuki H, Oba A, et al. Genetic dissection of medial habenula-interpeduncular nucleus pathway function in mice. Front Behav Neurosci. 2013;7:17.
10. Pergola G, Selvaggi P, Trizio S, Bertolino A, Blasi G. The role of the thalamus in schizophrenia from a neuroimaging perspective. Neurosci Biobehav Rev. 2015;54:57-75.
11. Cadigan KM, Waterman ML. TCF/LEFs and Wnt signaling in the nucleus. Cold Spring Harb Perspect Biol. 2012;4(11).
12. Hansen T, Ingason A, Djurovic S, Melle I, Fenger M, Gustafsson O, et al. At-risk variant in TCF7L2 for type II diabetes increases risk of schizophrenia. Biol Psychiatry. 2011;70(1):59-63.
13. Alkelai A, Greenbaum L, Lupoli S, Kohn Y, Sarner-Kanyas K, Ben-Asher E, et al. Association of the type 2 diabetes mellitus susceptibility gene, TCF7L2, with schizophrenia in an Arab-Israeli family sample. PLoS One. 2012;7(1):e29228.
14. Iossifov I, O'Roak BJ, Sanders SJ, Ronemus M, Krumm N, Levy D, et al. The contribution of de novo coding mutations to autism spectrum disorder. Nature. 2014;515(7526):216-21.
15. Winham SJ, Cuellar-Barboza AB, Oliveros A, McElroy SL, Crow S, Colby C, et al. Genome-wide association study of bipolar disorder accounting for effect of body mass index identifies a new risk allele in TCF7L2. Mol Psychiatry. 2014;19(9):1010-6.
16. Liu L, Li J, Yan M, Chen J, Zhang Y, Zhu X, et al. TCF7L2 polymorphisms and the risk of schizophrenia in the Chinese Han population. Oncotarget. 2017;8(17):28614-20.
17. Savic D, Distler MG, Sokoloff G, Shanahan NA, Dulawa SC, Palmer AA, et al. Modulation ofTcf7l2 expression alters behavior in mice. PLoS One. 2011;6(10):e26897.
18. Misztal K, Brozko N, Nagalski A, Szewczyk LM, Krolak M, Brzozowska K, et al. TCF7L2 mediates the cellular and behavioral response to chronic lithium treatment in animal models. Neuropharmacology. 2017;113(Pt A):490-501.
19. Nagalski A, Irimia M, Szewczyk L, Ferran JL, Misztal K, Kuznicki J, et al. Postnatal isoform switch and protein localization of LEF1 and TCF7L2 transcription factors in cortical, thalamic, and mesencephalic regions of the adult mouse brain. Brain Struct Funct. 2013;218(6):1531-49.
20. Wisniewska MB, Misztal K, Michowski W, Szczot M, Purta E, Lesniak W, et al. LEF1/beta-catenin complex regulates transcription of the Cav3.1 calcium channel gene (Cacna1g) in thalamic neurons of the adult brain. J Neurosci. 2010;30(14):4957-69.
21. Merchán P, Bardet SM, Puelles L, Ferran JL. Comparison of Pretectal Genoarchitectonic Pattern between Quail and Chicken Embryos. Front Neuroanat. 2011;5:23.
22. Bluske KK, Kawakami Y, Koyano-Nakagawa N, Nakagawa Y. Differential activity of Wnt/beta-catenin signaling in the embryonic mouse thalamus. Dev Dyn. 2009;238(12):3297-309.
23. Lee M, Yoon J, Song H, Lee B, Lam DT, Baek K, et al. Tcf7l2 plays crucial roles in forebrain development through regulation of thalamic and habenular neuron identity and connectivity. Dev Biol. 2017;424(1):62-76.
24. Nagalski A, Puelles L, Dabrowski M, Wegierski T, Kuznicki J, Wisniewska MB. Molecular anatomy of the thalamic complex and the underlying transcription factors. Brain Struct Funct. 2016;221(5):2493-510.

25. Evangelio M, García-Amado M, Clascá F. Thalamocortical Projection Neuron and Interneuron Numbers in the Visual Thalamic Nuclei of the Adult C57BL/6 Mouse. Front Neuroanat. 2018;12:27.
26. Vue TY, Aaker J, Taniguchi A, Kazemzadeh C, Skidmore JM, Martin DM, et al. Characterization of progenitor domains in the developing mouse thalamus. J Comp Neurol. 2007;505(1):73-91.
27. Delogu A, Sellers K, Zagoraiou L, Bocianowska-Zbrog A, Mandal S, Guimera J, et al. Subcortical visual shell nuclei targeted by ipRGCs develop from a Sox14+-GABAergic progenitor and require Sox14 to regulate daily activity rhythms. Neuron. 2012;75(4):648-62.
28. Galceran J, Miyashita-Lin EM, Devaney E, Rubenstein JL, Grosschedl R. Hippocampus development and generation of dentate gyrus granule cells is regulated by LEF1. Development. 2000;127(3):469-82.
29. Lee JE, Wu SF, Goering LM, Dorsky RI. Canonical Wnt signaling through Lef1 is required for hypothalamic neurogenesis. Development. 2006;133(22):4451-61.
30. Armenteros T, Andreu Z, Hortigüela R, Lie DC, Mira H. BMP and WNT signalling cooperate through LEF1 in the neuronal specification of adult hippocampal neural stem and progenitor cells. Sci Rep. 2018;8(1):9241.
31. Wisniewska MB. Physiological role of β-catenin/TCF signaling in neurons of the adult brain. Neurochem Res. 2013;38(6):1144-55.
32. Bielen H, Houart C. The Wnt cries many: Wnt regulation of neurogenesis through tissue patterning, proliferation, and asymmetric cell division. Dev Neurobiol. 2014;74(8):772-80.
33. Chodelkova O, Masek J, Korinek V, Kozmik Z, Machon O. Tcf7L2 is essential for neurogenesis in the developing mouse neocortex. Neural Dev. 2018;13(1):8.
34. Newman EA, Wu D, Taketo MM, Zhang J, Blackshaw S. Canonical Wnt signaling regulates patterning, differentiation and nucleogenesis in mouse hypothalamus and prethalamus. Dev Biol. 2018;442(2):236-48.
35. Mattes B, Weber S, Peres J, Chen Q, Davidson G, Houart C, et al. Wnt3 and Wnt3a are required for induction of the mid-diencephalic organizer in the caudal forebrain. Neural Dev. 2012;7:12.
36. Hagemann AI, Scholpp S. The Tale of the Three Brothers - Shh, Wnt, and Fgf during Development of the Thalamus. Front Neurosci. 2012;6:76.
37. Braun MM, Etheridge A, Bernard A, Robertson CP, Roelink H. Wnt signaling is required at distinct stages of development for the induction of the posterior forebrain. Development. 2003;130(23):5579-87.
38. Bluske KK, Vue TY, Kawakami Y, Taketo MM, Yoshikawa K, Johnson JE, et al. β-Catenin signaling specifies progenitor cell identity in parallel with Shh signaling in the developing mammalian thalamus. Development. 2012;139(15):2692-702.
39. Zhou CJ, Pinson KI, Pleasure SJ. Severe defects in dorsal thalamic development in low-density lipoprotein receptor-related protein-6 mutants. J Neurosci. 2004;24(35):7632-9.
40. Albuixech-Crespo B, López-Blanch L, Burguera D, Maeso I, Sánchez-Arrones L, Moreno-Bravo JA, et al. Molecular regionalization of the developing amphioxus neural tube challenges major partitions of the vertebrate brain. PLoS Biol. 2017;15(4):e2001573.
41. Echevarría D, Vieira C, Gimeno L, Martínez S. Neuroepithelial secondary organizers and cell fate specification in the developing brain. Brain Res Brain Res Rev. 2003;43(2):179-91.
42. Nakagawa Y, Shimogori T. Diversity of thalamic progenitor cells and postmitotic neurons. Eur J Neurosci. 2012;35(10):1554-62.
43. Husken U, Stickney HL, Gestri G, Bianco IH, Faro A, Young RM, et al. Tcf7l2 is required for left-right asymmetric differentiation of habenular neurons. Curr Biol. 2014;24(19):2217-27.
44. Price DJ, Clegg J, Duocastella XO, Willshaw D, Pratt T. The importance of combinatorial gene expression in early Mammalian thalamic patterning and thalamocortical axonal guidance. Front Neurosci. 2012;6:37.
45. Antón-Bolaños N, Espinosa A, López-Bendito G. Developmental interactions between thalamus and cortex: a true love reciprocal story. Curr Opin Neurobiol. 2018;52:33-41.
46. Hikosaka O, Sesack SR, Lecourtier L, Shepard PD. Habenula: crossroad between the basal ganglia and the limbic system. J Neurosci. 2008;28(46):11825-9.
47. Yuge K, Kataoka A, Yoshida AC, Itoh D, Aggarwal M, Mori S, et al. Region-specific gene expression in early postnatal mouse thalamus. J Comp Neurol. 2011;519(3):544-61.
48. Gezelius H, Moreno-Juan V, Mezzera C, Thakurela S, Rodríguez-Malmierca LM, Pistolic J, et al. Genetic Labeling of Nuclei-Specific Thalamocortical Neurons Reveals Putative Sensory-Modality Specific Genes. Cereb Cortex. 2017;27(11):5054-69.
49. Gezelius H, Lopez-Bendito G. Thalamic neuronal specification and early circuit formation. Dev Neurobiol. 2017;77(7):830-43.
50. Vue TY, Bluske K, Alishahi A, Yang LL, Koyano-Nakagawa N, Novitch B, et al. Sonic hedgehog signaling controls thalamic progenitor identity and nuclei specification in mice. J Neurosci. 2009;29(14):4484-97.

51. Scholpp S, Lumsden A. Building a bridal chamber: development of the thalamus. Trends Neurosci. 2010;33(8):373-80.
52. Quina LA, Wang S, Ng L, Turner EE. Brn3a and Nurr1 mediate a gene regulatory pathway for habenula development. J Neurosci. 2009;29(45):14309-22.
53. Suzuki-Hirano A, Ogawa M, Kataoka A, Yoshida AC, Itoh D, Ueno M, et al. Dynamic spatiotemporal gene expression in embryonic mouse thalamus. J Comp Neurol. 2011;519(3):528-43.
54. Nakagawa Y, O'Leary DD. Dynamic patterned expression of orphan nuclear receptor genes RORalpha and RORbeta in developing mouse forebrain. Dev Neurosci. 2003;25(2-4):234-44.
55. Nakagawa Y, O'Leary DD. Combinatorial expression patterns of LIM-homeodomain and other regulatory genes parcellate developing thalamus. J Neurosci. 2001;21(8):2711-25.
56. Mallika C, Guo Q, Li JY. Gbx2 is essential for maintaining thalamic neuron identity and repressing habenular characters in the developing thalamus. Dev Biol. 2015;407(1):26-39.
57. Li K, Zhang J, Li JY. Gbx2 plays an essential but transient role in the formation of thalamic nuclei. PLoS One. 2012;7(10):e47111.
58. Miyashita-Lin EM, Hevner R, Wassarman KM, Martinez S, Rubenstein JL. Early neocortical regionalization in the absence of thalamic innervation. Science. 1999;285(5429):906-9.
59. Chatterjee M, Li K, Chen L, Maisano X, Guo Q, Gan L, et al. Gbx2 regulates thalamocortical axon guidance by modifying the LIM and Robo codes. Development. 2012;139(24):4633-43.
60. Hevner RF, Miyashita-Lin E, Rubenstein JL. Cortical and thalamic axon pathfinding defects in Tbr1, Gbx2, and Pax6 mutant mice: evidence that cortical and thalamic axons interact and guide each other. J Comp Neurol. 2002;447(1):8-17.
61. Chen L, Guo Q, Li JY. Transcription factor Gbx2 acts cell-nonautonomously to regulate the formation of lineage-restriction boundaries of the thalamus. Development. 2009;136(8):1317-26.
62. Serrano-Saiz E, Leyva-Díaz E, De La Cruz E, Hobert O. BRN3-type POU Homeobox Genes Maintain the Identity of Mature Postmitotic Neurons in Nematodes and Mice. Curr Biol. 2018;28(17):2813-23.e2.
63. Vitalis T, Dauphinot L, Gressens P, Potier MC, Mariani J, Gaspar P. RORα Coordinates Thalamic and Cortical Maturation to Instruct Barrel Cortex Development. Cereb Cortex. 2017:1-14.
64. Ebisu H, Iwai-Takekoshi L, Fujita-Jimbo E, Momoi T, Kawasaki H. Foxp2 Regulates Identities and Projection Patterns of Thalamic Nuclei During Development. Cereb Cortex. 2016.
65. Beretta CA, Dross N, Bankhead P, Carl M. The ventral habenulae of zebrafish develop in prosomere 2 dependent on Tcf7l2 function. Neural Dev. 2013;8:19.
66. Vacik T, Stubbs JL, Lemke G. A novel mechanism for the transcriptional regulation of Wnt signaling in development. Genes Dev. 2011;25(17):1783-95.
67. Grindley JC, Hargett LK, Hill RE, Ross A, Hogan BL. Disruption of PAX6 function in mice homozygous for the Pax6Sey-1Neu mutation produces abnormalities in the early development and regionalization of the diencephalon. Mech Dev. 1997;64(1-2):111-26.
68. Lavado A, Lagutin OV, Oliver G. Six3 inactivation causes progressive caudalization and aberrant patterning of the mammalian diencephalon. Development. 2008;135(3):441-50.
69. Bulfone A, Puelles L, Porteus MH, Frohman MA, Martin GR, Rubenstein JL. Spatially restricted expression of Dlx-1, Dlx-2 (Tes-1), Gbx-2, and Wnt-3 in the embryonic day 12.5 mouse forebrain defines potential transverse and longitudinal segmental boundaries. J Neurosci. 1993;13(7):3155-72.
70. Fremeau RT, Troyer MD, Pahner I, Nygaard GO, Tran CH, Reimer RJ, et al. The expression of vesicular glutamate transporters defines two classes of excitatory synapse. Neuron. 2001;31(2):247-60.
71. Herzog E, Bellenchi GC, Gras C, Bernard V, Ravassard P, Bedet C, et al. The existence of a second vesicular glutamate transporter specifies subpopulations of glutamatergic neurons. J Neurosci. 2001;21(22):RC181.
72. Bibollet-Bahena O, Okafuji T, Hokamp K, Tear G, Mitchell KJ. A dual-strategy expression screen for candidate connectivity labels in the developing thalamus. PLoS One. 2017;12(5):e0177977.
73. Allen Institute for Brain Science. Allen Developing Mouse Brain Atlas. 2008 [Available from: http://developingmouse.brain-map.org/.
74. Lee S, Kohane I, Kasif S. Genes involved in complex adaptive processes tend to have highly conserved upstream regions in mammalian genomes. BMC Genomics. 2005;6:168.
75. Dabrowski M, Dojer N, Zawadzka M, Mieczkowski J, Kaminska B. Comparative analysis of cis-regulation following stroke and seizures in subspaces of conserved eigensystems. BMC Syst Biol. 2010;4:86.
76. Szabó NE, Zhao T, Zhou X, Alvarez-Bolado G. The role of Sonic hedgehog of neural origin in thalamic differentiation in the mouse. J Neurosci. 2009;29(8):2453-66.

77. Kiecker C, Lumsden A. Hedgehog signaling from the ZLI regulates diencephalic regional identity. Nat Neurosci. 2004;7(11):1242-9.
78. Hobert O. Regulatory logic of neuronal diversity: terminal selector genes and selector motifs. Proc Natl Acad Sci U S A. 2008;105(51):20067-71.
79. Liu C, Maejima T, Wyler SC, Casadesus G, Herlitze S, Deneris ES. Pet-1 is required across different stages of life to regulate serotonergic function. Nat Neurosci. 2010;13(10):1190-8.
80. Sunmonu NA, Li K, Guo Q, Li JY. Gbx2 and Fgf8 are sequentially required for formation of the midbrain-hindbrain compartment boundary. Development. 2011;138(4):725-34.
81. Cho EA, Dressler GR. TCF-4 binds beta-catenin and is expressed in distinct regions of the embryonic brain and limbs. Mech Dev. 1998;77(1):9-18.
82. Wisniewska MB, Nagalski A, Dabrowski M, Misztal K, Kuznicki J. Novel β-catenin target genes identified in thalamic neurons encode modulators of neuronal excitability. BMC Genomics. 2012;13:635.
83. Han S, Yang SH, Kim JY, Mo S, Yang E, Song KM, et al. Down-regulation of cholinergic signaling in the habenula induces anhedonia-like behavior. Sci Rep. 2017;7(1):900.
84. Ottschytsch N, Raes A, Van Hoorick D, Snyders DJ. Obligatory heterotetramerization of three previously uncharacterized Kv channel alpha-subunits identified in the human genome. Proc Natl Acad Sci U S A. 2002;99(12):7986-91.
85. Lebrand C, Cases O, Wehrlé R, Blakely RD, Edwards RH, Gaspar P. Transient developmental expression of monoamine transporters in the rodent forebrain. J Comp Neurol. 1998;401:506-24.
86. Persico AM, Mengual E, Moessner R, Hall FS, Revay RS, Sora I, et al. Barrel pattern formation requires serotonin uptake by thalamocortical afferents, and not vesicular monoamine release. J Neurosci. 2001;21(17):6862-73.
87. Bonnin A, Torii M, Wang L, Rakic P, Levitt P. Serotonin modulates the response of embryonic thalamocortical axons to netrin-1. Nat Neurosci. 2007;10(5):588-97.
88. Coutinho AM, Oliveira G, Morgadinho T, Fesel C, Macedo TR, Bento C, et al. Variants of the serotonin transporter gene (SLC6A4) significantly contribute to hyperserotonemia in autism. Mol Psychiatry. 2004;9(3):264-71.
89. Ansorge MS, Zhou M, Lira A, Hen R, Gingrich JA. Early-life blockade of the 5-HT transporter alters emotional behavior in adult mice. Science. 2004;306(5697):879-81.
90. Bright DP, Smart TG. Protein kinase C regulates tonic GABA(A) receptor-mediated inhibition in the hippocampus and thalamus. Eur J Neurosci. 2013;38(10):3408-23.
91. Choi S, Yu E, Lee S, Llinás RR. Altered thalamocortical rhythmicity and connectivity in mice lacking CaV3.1 T-type Ca2+ channels in unconsciousness. Proc Natl Acad Sci U S A. 2015;112(25):7839-44.
92. Hobert O. Terminal Selectors of Neuronal Identity. Curr Top Dev Biol. 2016;116:455-75.
93. Kadkhodaei B, Ito T, Joodmardi E, Mattsson B, Rouillard C, Carta M, et al. Nurr1 is required for maintenance of maturing and adult midbrain dopamine neurons. J Neurosci. 2009;29(50):15923-32.
94. Cave JW, Akiba Y, Banerjee K, Bhosle S, Berlin R, Baker H. Differential regulation of dopaminergic gene expression by Er81. J Neurosci. 2010;30(13):4717-24.
95. Lopes R, Verhey van Wijk N, Neves G, Pachnis V. Transcription factor LIM homeobox 7 (Lhx7) maintains subtype identity of cholinergic interneurons in the mammalian striatum. Proc Natl Acad Sci U S A. 2012;109(8):3119-24.
96. Skarnes WC, Rosen B, West AP, Koutsourakis M, Bushell W, Iyer V, et al. A conditional knockout resource for the genome-wide study of mouse gene function. Nature. 2011;474(7351):337-42.
97. Farley FW, Soriano P, Steffen LS, Dymecki SM. Widespread recombinase expression using FLPeR (flipper) mice. Genesis. 2000;28(3-4):106-10.
98. Taniguchi H, He M, Wu P, Kim S, Paik R, Sugino K, et al. A resource of Cre driver lines for genetic targeting of GABAergic neurons in cerebral cortex. Neuron. 2011;71(6):995-1013.
99. Allen Institute for Brain Science. Allen Mouse Brain Connectivity Atlas. Characterisation of Cck-IRES-Cre transgene. 2011 [Available from: http://connectivity.brain-map.org/transgenic/imageseries/list/1.html?gene_term=Cck-IRES-Cre.
100. Ferran JL, Ayad A, Merchán P, Morales- Delgado N, Sánchez-Arrones L, Alonso A, et al. Exploring Brain Genoarchitecture by Single and Double Chromogenic In Situ Hybridization (ISH) and Immunohistochemistry (IHC) on Cryostat, Paraffin, or Floating Sections. In Situ Hybridization Methods. Neuromethods. 99. 1 ed: Humana Press; 2015. p. 83-107.
101. Ferran JL, Ayad A, Merchán P, Morales- Delgado N, Sánchez-Arrones L, Alonso A, et al. Exploring Brain Genoarchitecture by Single and Double Chromogenic In Situ Hybridization (ISH) and Immunohistochemistry (IHC) in Whole-Mount Embryos. In Situ Hybridization Methods. Neuromethods. 99. 1 ed: Humana Press; 2015. p. 61-82.

102. Parrilla M, Chang I, Degl'Innocenti A, Omura M. Expression of homeobox genes in the mouse olfactory epithelium. J Comp Neurol. 2016;524(14):2713-39.
103. Chatterjee M, Guo Q, Weber S, Scholpp S, Li JY. Pax6 regulates the formation of the habenular nuclei by controlling the temporospatial expression of Shh in the diencephalon in vertebrates. BMC Biol. 2014;12:13.
104. Shimogori T, Lee DA, Miranda-Angulo A, Yang Y, Wang H, Jiang L, et al. A genomic atlas of mouse hypothalamic development. Nat Neurosci. 2010;13(6):767-75.
105. Walther C, Gruss P. Pax-6, a murine paired box gene, is expressed in the developing CNS. Development. 1991;113(4):1435-49.
106. Puelles L, Morales-Delgado N, Merchán P, Castro-Robles B, Martínez-de-la-Torre M, Díaz C, et al. Radial and tangential migration of telencephalic somatostatin neurons originated from the mouse diagonal area. Brain Struct Funct. 2016;221(6):3027-65.
107. Fedtsova NG, Turner EE. Brn-3.0 expression identifies early post-mitotic CNS neurons and sensory neural precursors. Mech Dev. 1995;53(3):291-304.
108. Kim D, Pertea G, Trapnell C, Pimentel H, Kelley R, Salzberg SL. TopHat2: accurate alignment of transcriptomes in the presence of insertions, deletions and gene fusions. Genome Biol. 2013;14(4):R36.
109. Anders S, Pyl PT, Huber W. HTSeq--a Python framework to work with high-throughput sequencing data. Bioinformatics. 2015;31(2):166-9.
110. Love MI, Huber W, Anders S. Moderated estimation of fold change and dispersion for RNA-seq data with DESeq2. Genome Biol. 2014;15(12):550.
111. Zhang Z, Wu H, Zhou H, Gu Y, Bai Y, Yu S, et al. Identification of potential key genes and high-frequency mutant genes in prostate cancer by using RNA-Seq data. Oncol Lett. 2018;15(4):4550-6.
112. Eden E, Navon R, Steinfeld I, Lipson D, Yakhini Z. GOrilla: a tool for discovery and visualization of enriched GO terms in ranked gene lists. BMC Bioinformatics. 2009;10:48.
113. Sunkin SM, Ng L, Lau C, Dolbeare T, Gilbert TL, Thompson CL, et al. Allen Brain Atlas: an integrated spatio-temporal portal for exploring the central nervous system. Nucleic Acids Res. 2013;41(Database issue):D996-D1008.
114. Krystkowiak I, Lenart J, Debski K, Kuterba P, Petas M, Kaminska B, et al. Nencki Genomics Database--Ensembl funcgen enhanced with intersections, user data and genome-wide TFBS motifs. Database (Oxford). 2013;2013:bat069.
115. Bray N, Dubchak I, Pachter L. AVID: A global alignment program. Genome Res. 2003;13(1):97-102.
116. Dabrowski M, Dojer N, Krystkowiak I, Kaminska B, Wilczynski B. Optimally choosing PWM motif databases and sequence scanning approaches based on ChIP-seq data. BMC Bioinformatics. 2015;16:140.

Figures

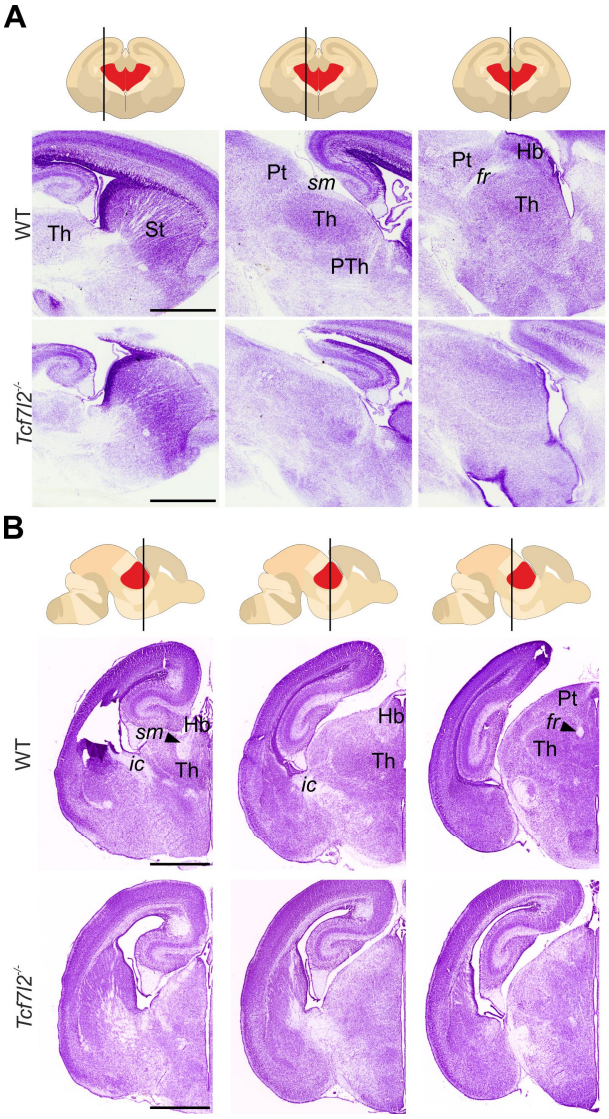

Fig. 1. **Histological analysis of brain anatomy.** (A) Nissl staining of sagittal brain sections on E18.5. (B) Nissl staining of coronal brain sections on P0 in the region of the diencephalon. In specimens from *Tcf7l2*$^{-/-}$ mice, the shape of the thalamic region is changed. The anatomical boundaries between the thalamus, prethalamus, habenula, and pretectum are not clearly visible. Cells do not cluster to form characteristic nuclei in the thalamus and habenula. The internal capsule is retained, but the stria medullaris cannot be easily identified, and the fasciculus retroflexus is not visible. Approximate planes of observation are marked by a black line on the

brain outlines. fr, fasciculus retroflexus; Hb, habenula; ic, internal capsule; Th, thalamus; Pt, pretectum; PTh, prethalamus; sm, stria medullaris; St, striatum. Scale bars represent 1 mm.

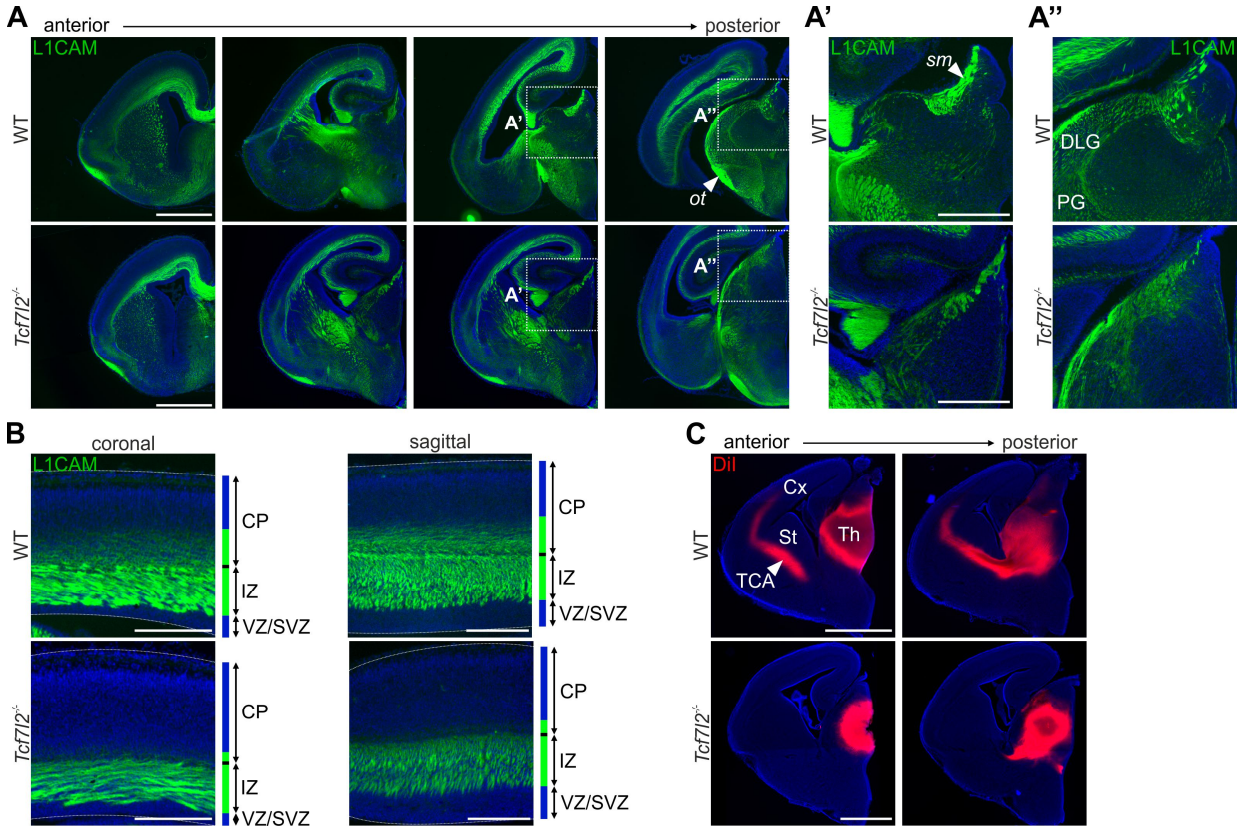

Fig. 2. **Staining of axon fascicles in the diencephalon on E18.5.** (A) Immunofluorescent staining of L1CAM in coronal brain sections. In specimens from *Tcf7l2*$^{-/-}$ mice, axons in thalamic and habenular areas are thinner and disorganised and there are fewer fascicles in the striatum. (A') and (A'') Zoomed-in views of the habenular region that show aberrant organisation of the stria medullaris in *Tcf7l2*$^{-/-}$ embryos. (B) Zoomed-in views of the cerebral cortex that show fewer axons that invade the cortical plate in *Tcf7l2*$^{-/-}$ embryos. (C) DiI tracing of thalamocortical tracts reveals little to no thalamocortical axon growth in *Tcf7l2*$^{-/-}$ embryos. Cx, cerebral cortex; CP, cortical plate; DLG, lateral geniculate nucleus; IZ, intermediate zone of the cortex; PG, pregeniculate nucleus; sm, stria medullaris; St, striatum; TCA thalamocortical axons; VZ/SVZ, ventricular zone and subventricular zone of the cortex. Scale bars represent 1 mm (A, C); 0.5 mm (A', A''); 0.25 mm (B).

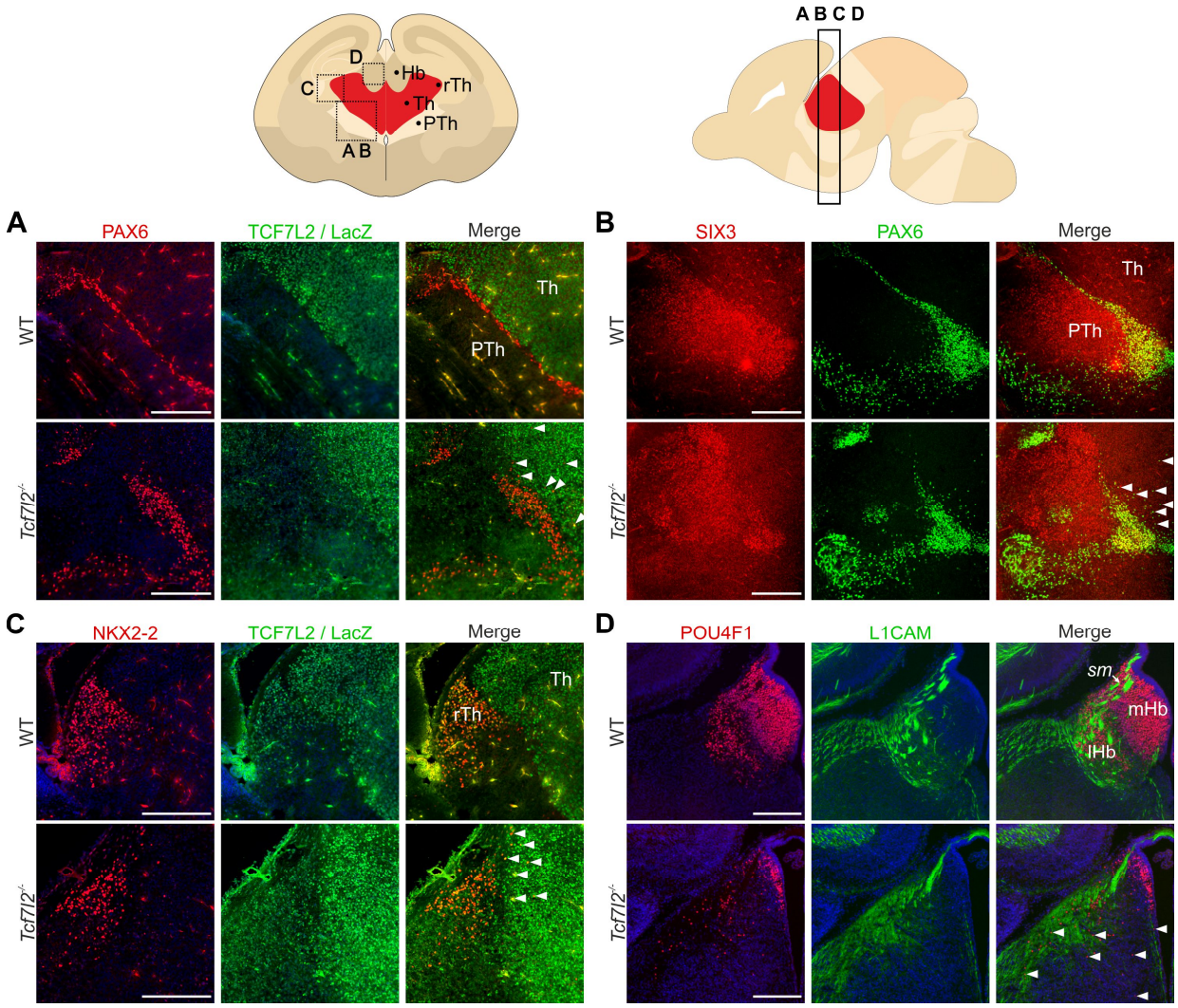

Fig. 3. **Analysis of anatomical borders of prosomere 2 on E18.5.** (A) Immunofluorescent staining of TCF7L2 (in wildtype) or LacZ (in *Tcf7l2*$^{-/-}$) and PAX6 in coronal brain sections. In specimens from *Tcf7l2*$^{-/-}$ mice, thalamo-prethalamic borders are not sharp and prethalamic cells (marked with white triangles) intermingle into the thalamic area. (B) Immunofluorescent staining of the prethalamic markers PAX6 and SIX3. PAX6-positive cells (marked with white triangles) invade the thalamus and the SIX3-positive area spreads into the thalamic region in *Tcf7l2*$^{-/-}$ embryos. (C) Immunofluorescent staining of TCF7L2/LacZ and the marker of the rTh NKX2-2. The borders between the caudal thalamus and rTh are not clear in *Tcf7l2*$^{-/-}$ embryos and an NKX2-

2-positive cells (marked with white arrows) intermingle into the caudal thalamus. (D) Immunofluorescent staining of the habenular marker POU4F1 and axonal marker L1CAM. The number of POU4F1-positive cells is reduced in the habenular region in *Tcf7l2*$^{-/-}$ embryos. The remaining POU4F1-positive cells either accumulate in the subventricular region of the habenula or spread into the thalamic area (marked with white arrows), which is not separated from the habenula by axon fascicles. Approximate fields of observation in the sagittal and coronal planes are marked by black boxes on the brain outlines above the photographs. Hb, habenula; lHb, lateral Hb; mHb, medial Hb; PTh, prethalamus; rTh, rostral thalamus, Th, thalamus. Scale bars represent 0.25 mm.

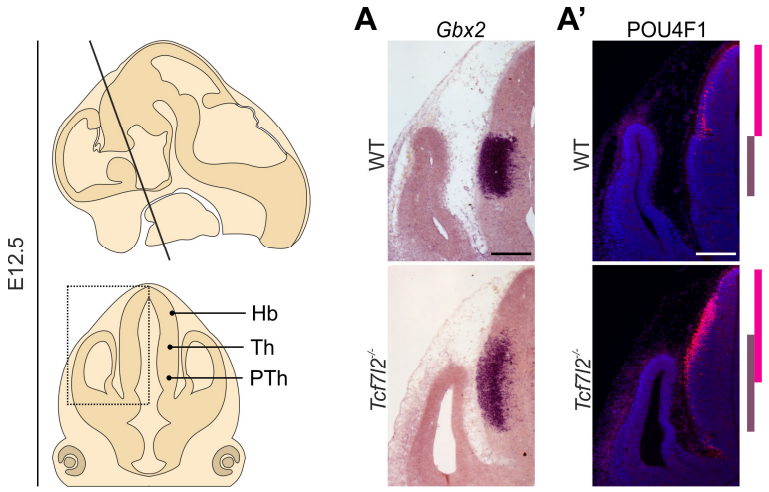

Fig. 4. **Analysis of thalamic and habenular molecular identities on E12.5.** (A) *In situ* hybridisation staining with a *Gbx2* probe (early marker of the thalamus) and (A') immunofluorescent staining of POU4F1 (early marker of the habenula) in coronal brain sections. In specimens from *Tcf7l2*$^{-/-}$ mice, both markers are normally expressed, but the *Gbx2*-positive region and POU4F1-positive region spread into each other's territory (emphasised by colored bars). Approximate fields of observation in the sagittal and coronal planes are marked by black boxes on the brain outlines above the photographs. Hb, habenula; PTh, prethalamus; Th, thalamus. Scale bars represent 0.25 mm.

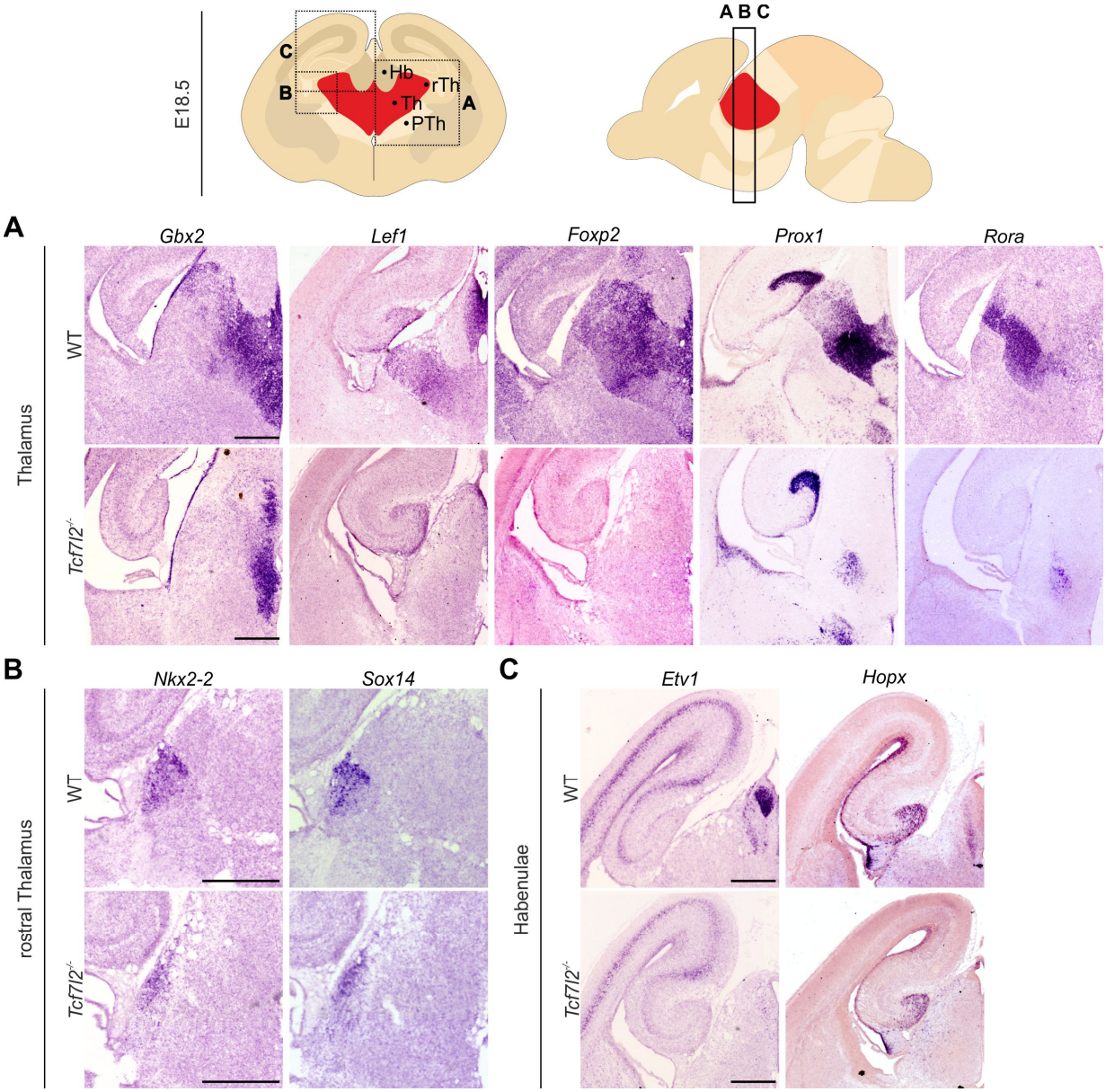

Fig. 5. **Analysis of thalamic and habenular molecular identities on E18.5.** (A) *In situ* hybridisation staining with *Gbx2, Lef1*, *Foxp2*, *Prox1* and *Rora* probes (markers of caudal thalamus regions) in coronal brain sections. In specimens from *Tcf7l2*$^{-/-}$ embryos, the expression of these markers is either abolished, or drastically reduced in area. (B) *In situ* hybridisation staining with *Nkx2-2* and *Sox14* probes (rTh markers). The expression of these markers is retained in *Tcf7l2*$^{-/-}$ embryos, although *Nkx2-2*- and *Sox14*-positive areas spread along the lateral wall of

the thalamic region. (C) *In situ* hybridisation staining with *Etv1* and *Hopx* probes (markers of the habenula). The expression of these markers is abolished in *Tcf7l2*$^{-/-}$ embryos. Approximate fields of observation in the sagittal and coronal planes are marked by black boxes on the brain outlines above the photographs. Hb, habenula; PTh, prethalamus; rTh, rostral thalamus; Th, thalamus. Scale bars represent 0.5 mm.

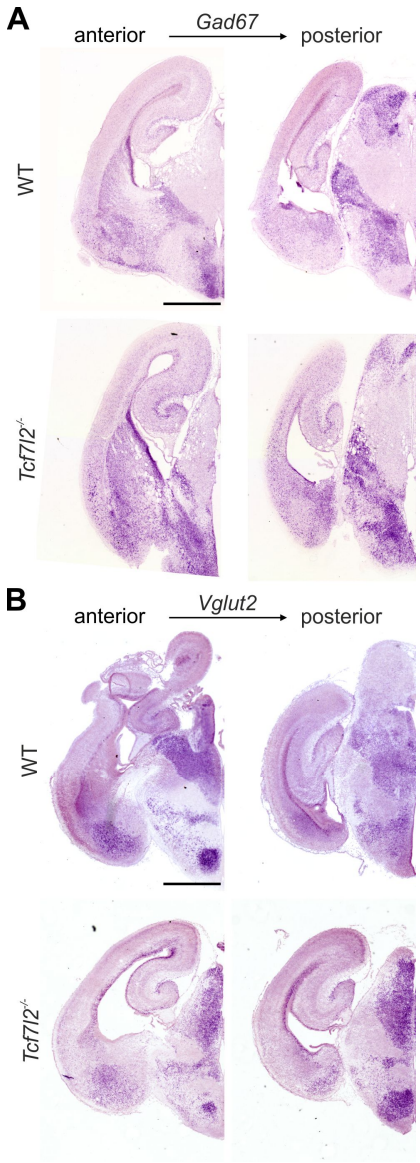

Fig. 6. **Analysis of neurotransmitter identity of neurons in the thalamo-habenular region on E18.5.** (A) *In situ* hybridisation staining with a *Gad67* probe (marker of GABAergic neurons) in coronal brain sections. (B) *In situ* hybridisation staining with a *Vglut2* probe (marker of glutamatergic neurons in prosomere 2). In specimens from *Tcf7l2*$^{-/-}$ mice, the thalamic area retains its predominant glutamatergic identity. Scale bars represent 1 mm.

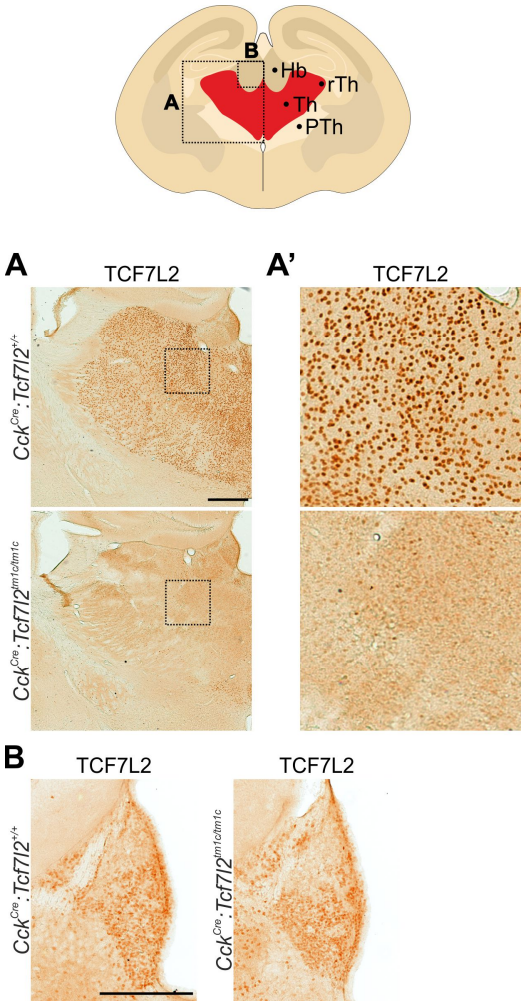

Fig. 7. **Characterisation of *Cck^{Cre}:Tcf7l2$^{tm1c/tm1c}$* mice.** (A) DAB immunohistochemical staining of TCF7L2 in coronal brain sections on P75. (A') Zoomed-in view on the thalamic area marked by black boxes on left panels. TCF7L2 is absent in most thalamic nuclei in adult *Cck^{Cre}:Tcf7l2$^{tm1c/tm1c}$* mice. (B) Zoomed-in view of the adult habenula, where TCF7L2 retains its presence in adult *Cck^{Cre}:Tcf7l2$^{tm1c/tm1c}$* mice. Approximate fields of observation are marked by black boxes on the brain outline above the photographs. Scale bars represent 0.5 mm (A); 0.25 mm (B).

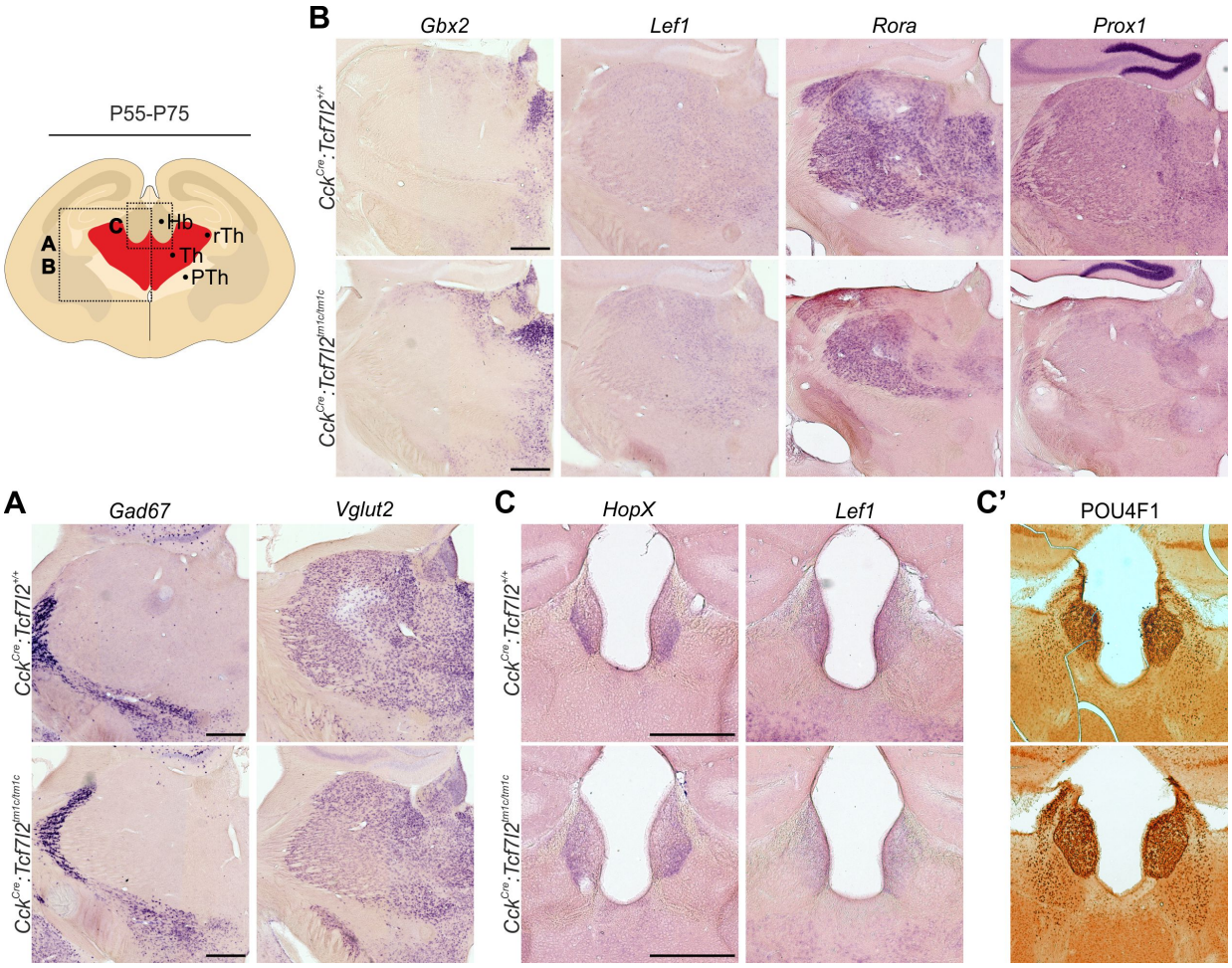

Fig. 8. **Analysis of thalamic and habenular molecular identities on ~P60.** (A) *In situ* hybridisation staining with a *Gad67* probe (marker of GABAergic neurons) and a *Vglut2* probe (marker of glutamatergic neurons). In specimens from *Cck*^{Cre}:*Tcf7l2*$^{tm1c/tm1c}$ mice, the thalamic area retains its glutamatergic identity. (B) *In situ* hybridisation staining with *Gbx2*, *Lef1*, *Rora* and *Prox1* probes (markers of thalamic subregions) in coronal brain sections. In specimens from *Cck*^{Cre}:*Tcf7l2*$^{tm1c/tm1c}$, the expression of *Gbx2* and *Lef1* shows little change. The expression of Rora is significantly lower in medial part of thalamus. The level of *Prox1* mRNA is also decreased. (C) *In situ* hybridisation staining with *Lef1* and *Hopx* probes (markers of habenular subregions), and (C') DAB immunohistochemical staining of the habenular marker POU4F1. The expression of these markers is retained in *Cck*^{Cre}:*Tcf7l2*$^{tm1c/tm1c}$ mice. Scale bars represent 0.5 mm.

Tables

Table 1. **Spatial expression profiles of down-regulated genes from selected GO clusters on E18.5.**

	Prosomere 2			Not in prosomere 2	Ubiquitous or low	NA
	Th	**Hb**	**Th and Hb**			
Transcription factors	*Hlf* *Foxp1* *Foxp2* *Gbx2** *Mef2a* *Mef2c* *Prox1* *Rora* *Rorb* *Sox13* *Sox5* *Tox* *Tshz1* *Zhx2*	*Dbx1* *Ebf1* *Nr4a2* *Pou4f1**	*Etv1* *Lef1* *Neurog2* *Tcf7L2*	*Esrrb*	*Esr2* *Grhl2* *Msx3* *Nr0b1* *Pparg*	*Aire* *Dmrta1* *Glis1* *Mecom* *Myocd* *Scrt1* *Scrt2* *Tbx5*
Adhesion/guiding molecules	*Cbln4* *Cd47* *Cdh6* *Cdh7* *Cdhr1* *Cntn6* *Epha1* *Epha3* *Epha4* *Ntng1* *Stxbp6* *Tgfb2*	*Robo3*	*Cdh8* *Epha8* *Kitl* *Rtn4rl1*	*Lama3*	*Dsc2* *Igsf5* *Scarf2*	*Cadm2* *Cntn4* *Col4a3* *Epcam* *Igsf21* *Lmo7* *Rgma* *Sema3g* *Slitrk6* *Tnfrsf12a* *Thy1*
Neural excitability	*Camk4* *Grik3* *Slc6a4*	*Chrnb4* *Gpr151* *Kcng4*	*Slc17a7*	*Drd1*	*Adra2b* *Drd4*	*Cacng1* *Grid2ip* *Homer2* *Kcnip4* *Kcnma1* *Kcnmb1* *Kcnq5* *Kcnv2* *Kntd6* *Shisa9* *Slc5a7* *Scn11a*

The listed genes were identified as down-regulated in prosomere 2 in *Tcf7l2*$^{-/-}$ embryos ($p < 0.05$; $\log_2$ fold-change < -0.5) and annotated into selected clusters. Spatial expression was analyzed in the ABA. Genes that are expressed distinctively higher in discrete parts of the brain were categorised as expressed in the thalamus (Th), habenula (Hb), both Th and Hb, or not expressed in prosomere 2. *, *Gbx2* and *Pou4f1* were not identified as differentially expressed based on RNA-seq but were added to the list based on *in situ* hybridization; NA, not available.

Table 2. **Spatial expression profiles of up-regulated genes from selected GO clusters on E18.5.**

	Prosomere 2			Not in prosomere 2	Ubiquitous or low	NA
	Th	**Hb**	**Th and Hb**			
Transcription factors	*Nkx2-2**	*Barhl2*	*Otx2***	*Dmbx1*	*E2f8*	*Grhl3*
	*Sox14**	*Onecut1*		*Ebf3*	*Egr1*	*Olig3*
				En2	*Emx1*	
				Maf	*Foxa2*	
				Nkx6-2	*Lhx5*	
				Onecut2	*Neurog1*	
				Pou4f2	*Onecut3*	
				Rreb1	*Sp5*	
				Sall4	*Uncx*	
Adhesion/guiding molecules			*Reln***	*Unc5d*	*Bmp7*	*Adamts2*
					Col18a1	*Adamts7*
					Slit3	*Cd177*
					Uncx	*Cyp1b1*
						Lgals3bp
						Ly9
						Mpz
						Pcdh8
						Serpinb8
						Svep1
Neural excitability				*Cacna2d1*	*Htr2a*	*Adra1d*
				Chrnb3		*Adrb3*
				Kcnip2		*Kcng3*
						Kcnk9
						Scn11a

The listed genes were identified as up-regulated in prosomere 2 in *Tcf7l2*$^{-/-}$ embryos ($p < 0.05$; $\log_2$ fold-change > 0.5) and annotated into selected clusters. Spatial expression was analyzed in the ABA. Genes that are expressed distinctively higher in discrete parts of the brain were categorised as expressed in the thalamus (Th), habenula (Hb), both Th and Hb, or not expressed in prosomere 2. * Expressed in the rTh; **, Expressed in the rTh and habenula; NA, not available.

Table 3. **Spatial expression profiles of down-regulated genes in selected GO clusters on P60.**

	Th	**Th and Hb**	**Not in Th**	**Ubiquitous or low**	**NA**
Ion channels/ pumps and homeostasis	*Kcnc2*	*Cacna1g* *Fxyd7*	*Kcnip3* *Hcn4*	*Cacna1s* *Cacna2d4* *Kcnf1* *Trpv6*	
Neurotransmitter receptors and transporters			*Cnih3*	*Adrb1*	*Adra1b*
G-protein signalling - other	*Atp2a1* *Atp2b1* *Gpr12* *Rims3*	*Gpr153*	*Atp2a3* *Gpr4*	*Gpr35* *Gpr115* *Gpr133* *F2r* *Rgs7* *Gpr111*	
Synaptic vesicle regulation		*Syt9* *Syt7*			
Excitability and plasticity- other	*Bdnf* *Cnksr3* *Shisa6* *Trpm6*	*Calb1* *Pcp4*		*Orai3* *Shank3* *Slc12a8*	

The listed genes were identified as down-regulated in the thalamo-habenular region in *Cck*^{Cre}:*Tcf7l2*$^{tm1c/tm1c}$ mice ($p < 0.05$; $\log_2$ fold-change < -0.5) and annotated into selected clusters. Spatial expression was analyzed in the ABA. Genes that are expressed distinctively higher in discrete parts of the brain were categorised as expressed in the thalamus (Th), thalamus and habenula (Hb), or not expressed in the thalamus. NA, not available.

Table 4. **Spatial expression profiles of up-regulated genes in selected GO clusters on P60.**

	Th	**Th and Hb**	**Not in Th**	**Ubiquitous or low**	**NA**
Voltage-gated ion channels	*Scn4b*		*Hcn1* *Kcnh3* *Kcnh7* *Kcns3* *Kcnip2* *Cacna1i*	*Kcnc3* *Kcne4* *Kcnk4*	*Kcns1* *Trpv3*
Neurotransmitter receptors	*Glra1*		*Adra1d* *Htr1b* *Gsg1l*	*Glra2*	
G-protein signalling - other			*Npy5r*	*Gpr149*	
Synaptic vesicle regulation			*Cplx2*	*Cplx3* *Snap25* *Syt2*	
Excitability and plasticity - other			*Pln*	*Prkg2* *Pvalb* *Sgk1* *Stac2*	*Efcab4b*

The listed genes were identified as up-regulated in the thalamo-habenular region in *Cck*^{Cre}*:Tcf7l2*$^{tm1c/tm1c}$ mice ($p < 0.05$; $\log_2$ fold-change > 0.5). Spatial expression was analysed in the ABA. Genes that are expressed distinctively higher in discrete parts of the brain were categorised as expressed in the thalamus (Th), thalamus and habenula (Hb), or not expressed in the thalamus. NA, not available.

Additional files

Additional file 1.pdf

Supplementary figures:

Fig. S1. **Generation and characterisation of the homozygous *Tcf7l2^{tm1a}* mouse strain (*Tcf7l2$^{-/-}$*).** (A) Schematic representation of *Tcf7l2^{tm1a}* allele generated by EUCOMM, in which a trap cassette with the LacZ and neoR elements was inserted upstream of the critical exon 6 of the *Tcf7l2* gene. Exons and introns are represented by vertical black and horizontal gray lines, respectively. Blue arrows indicate transcription start sites. The regions that encode the β-catenin binding domain and HMG-box are marked by red lines above the exons. (B) Immunofluorescent staining of TCF7L2 in coronal and sagittal brain sections on E18.5. The expression of TCF7L2 protein is lost in *Tcf7l2$^{-/-}$* mice. (C) Western blot analysis of TCF7L2 protein expression in the thalamus in wild-type and *Tcf7l2$^{-/-}$* mice on E18.5. Higher TCF7L2 bands correspond to the full-length protein, and the lower bands correspond to the truncated dominant negative isoform of TCF7L2 (dnTCF7L2). Scale bars represent 1 mm.

Fig. S2. **Neurogenesis in prosomere 2 on E12.5.** Immunofluorescent staining of the proliferation marker KI-67 antigen and neural marker TUJ1 (neuron-specific class III β-tubulin) in coronal brain sections. Proliferating cells are visible along the ventricle, and young neurons are visible in the mantle zone, both in WT and *Tcf7l2$^{-/-}$* embryos.

Fig. S3. **Expression of *Tcf7l2* mRNA throughout the diencephalon.** *In situ* hybridization staining with a *Tcf7l2* probe on E18.5. *Tcf7l2* expression marks the thalamus, habenula, and pretectum. Specific cell densities allow the discernment of different thalamic nuclei and the medial and lateral habenula. Although *Tcf7l2* mRNA is detected in knockout mice, the characteristic anatomy of all of the shown regions and cell densities of specific nuclei are not preserved.

Fig. S4. **Genome-wide analysis of gene expression (RNA-seq) in the thalamo-habenular region.** (A) Scatter plot of $\log_2$ average expression levels of genes in WT embryos on E18.5 vs. $\log_2$ fold-change in the knockout condition. (B) Volcano plot of $\log_2$ fold-change of expression between WT and *Tcf7l2*$^{-/-}$ embryos vs. $-\log_{10}$ p values (Student's t-test) of the difference. (C) Scatter plot of $\log_2$ average expression levels of genes in P60 *Cck*^{Cre}*:Tcf7l2*$^{+/+}$ vs. $\log_2$ fold-change in the *Cck*^{Cre}*:Tcf7l*$^{tm1c/tm1c}$ knockout condition. (D) Volcano plot of $\log_2$ fold-change of expression between P60 *Cck*^{Cre}*:Tcf7l2*$^{+/+}$ and *Cck*^{Cre}*:Tcf7l*$^{tm1c/tm1c}$ mice vs. $-\log_{10}$ p values (Student's t-test) of the difference. Genes that significantly increased or decreased ($p < 0.05$, absolute $\log_2$ fold-change > 0.5) are marked as red.

Additional file 2.pdf

Supplementary tables:

Table S2. **Clusters of highly enriched gene ontology terms in differentially expressed gens on E18.5** Genes that were identified as significantly increased or decreased in the thalamo-habenular region in *Tcf7l2*$^{-/-}$ embryos were analysed with GOrilla. GO, gene ontology number; Hits, number of genes in a cluster; FDR, false discovery rate.

Table S7. **Clusters of highly enriched gene ontology terms in differentially expressed gens on ~P60** Genes that were identified as significantly increased or decreased in the thalamo-habenular region in *Cck*^{Cre}*:Tcf7l2*$^{tm1c/tm1c}$ mice were analysed with GOrilla. GO, gene ontology number; Hits, number of genes in a cluster; FDR, false discovery rate.

Table S10. **Probes and primers used in the study**

Additional file 3.xlsx

Supplementary Table S1:

Table S1. **RNA-seq analysis of differential gene expression in prosomere 2 between WT and *Tcf7l2*$^{-/-}$ mice on E18.5**

The experiment was performed in three replicates for WT and *Tcf7l2*$^{-/-}$ mice. All genes that lacked RPKM counts for all replicates were discarded. Average RPKM, fold-change, and $\log_2$ fold-change were calculated for WT and KO samples. Two-tailed Student's t-tests were performed to determine significance of the fold-changes. Genes with log2 fold-changes > 0.5 and $p < 0.05$ were assigned as differentially expressed.

Additional file 4.xlsx

Supplementary Table S3:

Table S3. **GO term analysis of differentially regulated genes in prosomere 2 in *Tcf7l2*$^{-/-}$ mice on E18.5**

Significantly up- and down-regulated genes were fed as targets in the Gorilla tool, with unchanged genes as controls. The tool was used to discover enriched terms for biological processes and molecular function.

Additional file 5.xlsx

Supplementary Table S4:

Table S4. **Spatial expression profiles of differentially expressed genes from selected GO clusters on E18.5**

Spatial expression profiles in the brain of GO-enriched genes that were differentially expressed in *Tcf7l2*$^{-/-}$ mice (absolute $\log_2$ fold-change > 0.5, p-value < 0.5) and analysed visually in the ABA on E18.5. The expression of each gene was categorised as specific for prosomere 2 (Th and/or Hb), other regions beyond prosomere 2, or ubiquitous. "0" represents ubiquitous or no expression in the brain; "+" represents higher expression in a particular region in comparison to other regions in the brain; analysed visually in ABA on E18.5

Additional file 6.xlsx

Supplementary Table S5:

Table S5. **Motif enrichment analysis of differentially regulated genes in prosomere 2 in *Tcf7l2*$^{-/-}$ mice on E18.5**

The motifs were analysed in conserved non-coding regions within ± 10 Kb from transcription start sites. Significance was calculated using Fisher's exact test, and p values were Bonferroni-corrected.

Additional file 7.xlsx

Supplementary Table S6:

Table S6. **RNA-seq analysis of differential gene expression in prosomere 2 between WT and *Cck^{Cre}:Tcf7l2$^{tm1c/tm1c}$* mice on P60**

The experiment was performed in three replicates for WT and *Cck^{Cre}:Tcf7l2$^{tm1c/tm1c}$* mice. All genes that lacked RPKM counts for all replicates were discarded. Average RPKM, fold-change, and $\log_2$ fold-change were calculated for WT and KO samples. Two-tailed Student's t-tests were performed to determine significance of the fold-changes. Genes with absolute $\log_2$ fold-changes > 0.5 and $p < 0.05$ were assigned as differentially expressed.

Additional file 8.xlsx

Supplementary Table S8:

Table S8. **GO term analysis of differentially regulated genes in the thalamo-habenular region in *Cck^{Cre}:Tcf7l2$^{tm1c/tm1c}$* mice on P60**

Significantly up- and down-regulated genes were fed as targets in the Gorilla tool, with unchanged genes as controls. The tool was used to discover enriched terms for biological processes and molecular function.

Additional file 9.xlsx

Supplementary Table S9:

Table S9. **Spatial expression profiles of differentially expressed genes from selected GO clusters on P60**

Spatial expression profiles in the brain of GO-enriched genes that were differentially expressed in *Cck*^{Cre}*:Tcf7l2*$^{tm1c/tm1c}$ mice on P60 (absolute $\log_2$ fold-change > 0.5, p-value < 0.5) and analysed visually in the ABA on P56. The expression of each gene was categorised as specific for the thalamus or thalamus and habenula, other regions beyond prosomere 2, or ubiquitous. "0" represents ubiquitous or no expression in the brain; "+" represents higher expression in a particular region in comparison to other regions in the brain; analysed visually in ABA on E18.5